AD-A286 162

DEVELOPMENT OF LIGHTWEIGHT TITANIUM BASE ALLOYS

R.J. Lederich, T.C. Peng, J.E. O'Neal, D.S. Schwartz, J.E. Deffeyes, and
S.M.L. Sastry
McDONNELL DOUGLAS RESEARCH LABORATORIES
P.O. BOX 516
ST. LOUIS, MO 63166

DTIC
ELECTE
NOV 15 1994
S B D
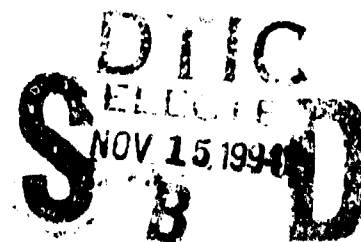
15 APRIL 1989

FINAL REPORT
Period Covering 12 September 1986 to 12 April 1989

Approved for Public Release; Distribution is Unlimited.

94-35251

94 111 063

NOTICES

REPORT NUMBERING SYSTEM — The numbering of technical project reports issued by the Naval Air Warfare Center, Aircraft Division, Warminster is arranged for specific identification purposes. Each number consists of the Center acronym, the calendar year in which the number was assigned, the sequence number of the report within the specific calendar year, and the official 2-digit correspondence code of the Functional Department responsible for the report. For example: Report No. NAWCADWAR-92001-60 indicates the first Center report for the year 1992 and prepared by the Air Vehicle and Crew Systems Technology Department. The numerical codes are as follows:

CODE	OFFICE OR DEPARTMENT
00	Commanding Officer, NAWCADWAR
01	Technical Director, NAWCADWAR
05	Computer Department
10	AntiSubmarine Warfare Systems Department
20	Tactical Air Systems Department
30	Warfare Systems Analysis Department
50	Mission Avionics Technology Department
60	Air Vehicle & Crew Systems Technology Department
70	Systems & Software Technology Department
80	Engineering Support Group
90	Test & Evaluation Group

PRODUCT ENDORSEMENT — The discussion or instructions concerning commercial products herein do not constitute an endorsement by the Government nor do they convey or imply the license or right to use such products.

Reviewed By: _William Frazier for Al New_   Date: _8/1/94_

Contracting Officer's Technical Representative (COTR)
or
Point Of Contact (POC)

Reviewed By: _J. Waldman_   Date: _8/2/94_

Branch Head

Reviewed By: _Irving S. Shaffer_   Date: _8/3/94_

Division Head

REPORT DOCUMENTATION PAGE

1. AGENCY USE ONLY (Leave blank)	2. REPORT DATE 15 APRIL 1983	3. REPORT TYPE AND DATES COVERED FINAL 9/12/86 – 4/12/89

4. TITLE AND SUBTITLE

DEVELOPMENT OF LIGHTWEIGHT TITANIUM BASE ALLOYS

5. FUNDING NUMBERS

N62269-86-C-0262

6. AUTHOR(S)

R.J. LEDERICH, T.C. PENG, J.E. O'NEAL, D.S. SCHWARTZ, J.E. DEFFEYES, and S.M.L. SASTRY

7. PERFORMING ORGANIZATION NAME(S) AND ADDRESS(ES)

McDONNELL DOUGLAS RESEARCH LABORATORIES
P.O. BOX 516
ST LOUIS, MO 63166

8. PERFORMING ORGANIZATION REPORT NUMBER

MDC QA028

9. SPONSORING / MONITORING AGENCY NAME(S) AND ADDRESS(ES)

Air Vehicle and Crew Systems Technology Department (Code 6063)
NAVAL AIR WARFARE CENTER; AIRCRAFT DIVISION WARMINSTER
P.O. Box 5152
Warminster, PA 18974-0591

10. SPONSORING / MONITORING AGENCY REPORT NUMBER

NAWCADWAR-94098-60

11. SUPPLEMENTARY NOTES

NAWCADWAR P.O.C. — William Frazier, Ph.D. — Code 6063

12a. DISTRIBUTION / AVAILABILITY STATEMENT

APPROVED FOR PUBLIC RELEASE; DISTRIBUTION IS UNLIMITED.

12b. DISTRIBUTION CODE

13. ABSTRACT (Maximum 200 words)

The goal of the program on Development of Lightweight Titanium Base Alloys was to develop new titanium alloys with 10% lower density, 50% higher elastic modulus, and 50% higher strength than Ti-6Al-4V and a 150°C increase in service temperature above that of Ti-6Al-2Sn-4Zr-2Mo. The feasibility of adding significant amounts of Be, Li, and Mg to Ti base alloys to effect these improvements was investigated. Rapid solidification processing was employed to obtain extended solid solutions of Be concentrations far exceeding the limits indicated by the equilibrium phase diagram. This solid solution was expected to provide significant strengthening because of the atomic-radius mismatch between Ti and solute atoms, and to provide dispersion strengthening via fine dispersions.

Master alloys of Ti-Al-Be and Ti-V-Al-Be were produced by melting pieces of Lockalloy (60 wt%) Be – 40 wt% Al) and elemental additions in a Beo-wash-coated alumina crucible, and casting at 1450°C into a chilled mold. Powder was produced by melting the master alloys in an uncoated graphite crucible, initiating metal flow at 1300°C, and dispersing the stream by centrifugal atomization. Target alloy chemistries were obtained, although the powders contained 0.5–0.7 wt% oxygen. This oxygen pickup occurred during

14. SUBJECT TERMS		15. NUMBER OF PAGES
		16. PRICE CODE

17. SECURITY CLASSIFICATION OF REPORT	18. SECURITY CLASSIFICATION OF THIS PAGE	19. SECURITY CLASSIFICATION OF ABSTRACT	20. LIMITATION OF ABSTRACT
UNCLASSIFIED	UNCLASSIFIED	UNCLASSIFIED	SAR

casting and is attributed to the BeO wash and/or the relatively poor vacuum. The powders were extruded into 12-cm diameter rods at 900 and 950°C (except Ti-34A1-4Be which was extruded at 1150°C). Successful extrusions were obtained for Ti-6Al-4V-4Be, Ti-6Al-4V-7Be, Ti-25V-3Al-4Be, Ti-25V-4Ai-7Be, and Ti-34Al-4Be.

The Ti-6Al-4V-4Be alloy has a single-phase microstructure and contains a fine, uniform dispersion of $TiBe_2$. The Ti-25V-4Al-7Be alloy has a two-phase microstructure containing 3-µm-diameter grains. The continuous phase is enriched with V, but does not contain Be. The discontinous phase, which contains 50 at.% Be, also has a fine dispersion of TiB_2.

The Ti-6Al-4V-xBe and Ti-25V-xBe alloys were machinable by conventional techniques. The densities of the extrusions were from 3.4 to 19% lower than that of Ti-6Al-4V. Dynamic moduli at 25°C were 159 Gpa for Ti-6Al-4V-7Be, 137 Gpa for Ti-25V-4Al-7Be, and 194 Gpa for Ti-34Al-4Be, which are improvements of 15–45% over the base alloys. Of the heat-treatments investigated, 1000°C/20 h yielded the best mechanical properties. Compressive flow stresses of 1000 MPa (145 ksi) at 700°C and 415 MPa (60 ksi) at 185°C were measured for Ti-6Al-4V-7Be. Strengths of this alloy exceed reported values for TiAl and Ti_3Al alloys at temperatures lower than 800°C. The other alloys were comparably strengthened. Fracture thoughness values of 19 $MPa(m)^{1/2}$ were obtained for the Ti-25V-4Al-7Be alloy.

Attempts to produce rapidly solidified Ti-Al-Li and Ti-Al-Mg were unsuccessful because of excessive vaporization of Li and Mg at the temperatures required for melting and atomization of Ti alloys.
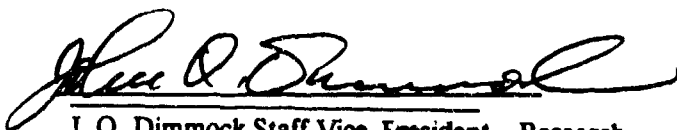
PREFACE

This report was prepared by the McDonnell Douglas Research Laboratories (MDRL), St. Louis, MO, for the Naval Air Development Center (NADC), Warminster, PA, under Contract N62269-86-C-0262. The NADC Program Manager was C. Edward Neu.

The work was performed in the Solid State Sciences Department of MDRL under the supervision of Dr. C. R. Whitsett. The principal investigator was Dr. S. M. L. Sastry; co-investigators were Mr. R. J. Lederich, Dr. T. C. Peng, Mr. J. E. O'Neal, Dr. D. S. Schwartz, and Dr. J. E. Deffeyes.

This report has been reviewed and is approved.

C. R. Whitsett Director – Research
McDonnell Douglas Research Laboratories

J. O. Dimmock Staff Vice-President – Research
McDonnell Douglas Research Laboratories

TABLE OF CONTENTS

LIST OF ILLUSTRATIONS

LIST OF ILLUSTRATIONS

(continued)

LIST OF TABLES

LIST OF TABLES

(continued)

1. INTRODUCTION

The objective of the program on Development of Lightweight Titanium Base Alloys is to develop practical lightweight titanium alloys for use in advanced Naval aircraft structures and propulsion systems. These alloys should possess significantly better mechanical properties on a density-normalized basis than current structural and propulsion titanium alloys and be suitable for use at higher service temperatures. The specific property-improvement goals were 10% lower density, 50% higher elastic modulus, and 50% higher strength than Ti–6Al–4V and a 150°C increase in service temperature above that of Ti–6Al–2Sn–4Zr–2Mo.

Alpha–based Ti–6Al–4V, with its excellent combination of strength and fracture toughness, and Ti–25V–based beta alloys, with their high strengths and ductilities, were selected as base alloy compositions. After the program began, the gamma–Ti–35Al alloy was added. The principal thrust was to add significant amounts of Be to these base alloys by rapid solidification processing (RSP). Beryllium substantially decreases the density of the alloy, provides substantial solid–solution strengthening because of its atomic radius mismatch with titanium, and provides dispersion strengthening by $TiBe_2$ dispersoids. Rapid solidification processing is necessary to exceed the equilibrium solid solubility (1 wt% Be in beta Ti and 0.2 wt% Be in alpha Ti) and to avoid segregation. Additions of small amounts of B, C, Si, and Er_2O_3 were made to the base alloys to produce further increases in strength, modulus, and creepresistance at high temperatures.

A secondary thrust of this program was to add Li and Mg to the base alloys in sufficient concentrations to decrease overall alloy densities by 10% or more. The volatility of Mg and Li at the melting temperature of Ti required the exploration of innovative melting techniques.

The approach of this program was to produce rapidly solidified powders by an appropriate technique, consolidate powders to fully dense bars, evaluate mechanical properties, and correlate the mechanical properties with microstructures.

2. RESEARCH OBJECTIVES AND APPROACH

The overall objectives of this program established by MDRL were to (1) produce RSP powders of alloys of Ti-6Al-4V and Ti-25V containing varying amounts of Be, Li, Mg, B, C, Si, and Er_2O_3 ; (2) consolidate these alloys to fully dense rods; (3) evaluate the mechanical properties of these alloys after suitable heat-treatments; and (4) correlate the mechanical properties with the alloy microstructures. The research described in this report was conducted under six tasks.

Task 1: Alloy Selection and Preparation

Eleven titanium-based alloys containing two concentration levels of Be with and without small amounts of B, C, Si, and Er_2O_3 were chosen. Seven master alloy ingots were successfully cast.

Task 2: Rapid Solidification Processing

7-kg castings served as the charge for rapid solidification rate (RSR) powder production. Powders of six alloys were successfully produced with yields varying between 435 and 1705 grams.

Task 3: Consolidation and Thermomechanical Processing

All six alloys were extruded into 13-mm- (0.5-in.) diameter bars. Extrusion ratios were approximately 13:1 and two extrusion temperatures were used for most alloys. Extrusions were given two different heat-treatments in preparation for mechanical property evaluation.

Task 4: Microstructural Characterization

Scanning electron microscopy, Auger electron spectroscopy, and transmission electron microscopy were employed to determine the microstructures, identify the different phases, and characterize the fine dispersions in the Ti-6Al-4V- and Ti-25V-based alloys.

Task 5: Mechanical Property Evaluation

The density and dynamic modulus were determined for each class of alloys. Elevated-temperature tensile and compressive strengths and creep properties were determined for these alloys in the as-extruded and heat-treated conditions. The fracture toughness of the beta alloys was determined.

Task 6: Alloy Assessment

The evaluated alloys were assessed by comparing their properties with the program goals.

3. SELECTION AND RAPID SOLIDIFICATION PROCESSING OF BERYLLIUM-CONTAINING TITANIUM ALLOYS

3.1 Alloy Selection

The 11 beryllium-containing titanium alloys investigated in this study are listed in Table 1. Alloys 1-5 are variations of the α/β alloy Ti-6Al-4V, which is used extensively in Navy aircraft structural applications. These compositions were chosen to investigate the effects of two different levels of Be additions as well as the effects of B, C, Si, and Er_2O_3 additions. Alloys 6-10 are variations of the ductile β Ti-26V alloy, which has high strength and is formable at room temperature. These β alloys also contain two levels of Be additions, as well as B, C, Si, and Er_2O_3. Alloy 11, which was added after the start of this program, permitted the evaluation of a low-density, dispersion-strengthened $\alpha_2 + \gamma$ titanium aluminide, which has excellent high temperature strength and oxidation resistance.

Table 1. Ti-Al-Be alloys selected for this study.

No.	Alloy
1	Ti-6Al-4V-2.75Be
2	Ti-6Al-4V-2.75Be-2Er$_2$O$_3$
3	Ti-6Al-4V-2.75Be-1B-1C-1Si
4	Ti-6Al-4V-5.5Be
5	Ti-6Al-4V-5.5Be-1B-1C-1Si
6	Ti-26V-2.75Be-.75Al
7	Ti-26V-2.75Be-1B-1C-.75Al
8	Ti-26V-2.75Be-2Er$_2$O$_3$-.75Al
9	Ti-26V-5.5Be-1.5Al
10	Ti-26V-5.5Be-1B-1C-1.5Al
11	Ti-34Al-4Be

89-224-300a

3.2 Rapid Solidification Processing

The alloy powders were produced by the rapid-solidification-rate (RSR) process at Pratt and Whitney Aircraft, West Palm Beach, FL. The procedure consisted of heating the charge in an uncoated graphite crucible equipped with a graphite stopper rod, homogenizing the melt for approximately 5 minutes, raising the stopper rod to initiate metal flow, atomizing the melt stream with a 100-mm-diameter cup rotating at 19 000 rpm, and cooling the metal droplets with helium gas. The initial attempt was with Ti-6Al-4V-5.5Be (alloy 4), for which the charge consisted of chunks (-30-mm cubic dimensions) of Ti-6Al-4V and sections of 10-mm-diameter Lockalloy (60 wt% Be-40 wt% Al mastcralloy) rods. The Lockalloy melted and reacted with the graphite control rod which initiated flow before the Ti-6Al-4V pieces melted, and the material was scrapped.

A second atomization run was attempted with Ti-6Al-4V-2.5Be (alloy 1), but the Be reacted with the graphite crucible and opened leaks before the Ti-6Al-4V pieces melted. This material was also scrapped.

Based on the first two runs, it was concluded that prealloyed ingots were required. Advanced Metallurgy and Testing (AMT) Corporation, Reading, PA, was contracted to produce prealloyed ingots to serve as charges for the RSR atomization runs.

The experimental setup at AMT is shown in Figure 1. The Ti, small chunks of Lockalloy (60 wt% Be-40 wt% Al), and granules of boron, carbon, silicon, and erbium oxide were placed in a 150-mm- (6-in.) diame-

ter alumina crucible, which was coated with a BeO wash. The Lockalloy chunks were placed on top of the titanium so that they would dissolve into the titanium upon melting. The induction heated crucible was equipped with a removable top to facilitate temperature measurements with an optical pyrometer. The entire setup was housed inside a mechanically pumped vacuum system.

Removable top —

— Induction heated tilting crucible

— Chilled graphite mold

89-224-272
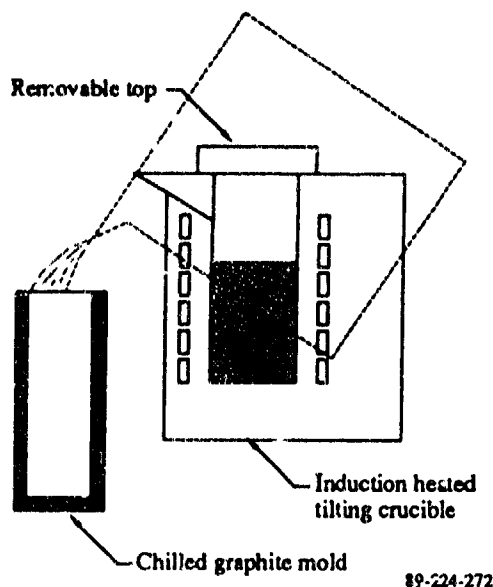
Figure 1. The experimental Ti-Be-alloy casting system at Advanced Metallurgy and Testing Corp.

The melt chamber was alternatively evacuated and backfilled with argon. The charge was heated under a vacuum of 40 Pa (0.3 Torr) at a rate of 35°C/min; when complete melting occurred, heating was continued to superheat the melt by about 125°C, after which the system was backfilled with Ar and the melt was poured into chilled graphite molds.

Castings were obtained for alloys 1, 4, 5, 6, 8, 9, and 11. The Lockalloy melted at ≈1195°C, in agreement with reported data. Complete melting occurred at around 1345°C, which is considerably lower than the melting temperature of titanium (1668°C). Material yields were greater than 95%, resulting in ingots weighing between 6 and 7.5 kg. The chemical analyses of the castings were performed by Analytical Associates of Detroit, MI. The seven castings were shipped to Pratt and Whitney Corp., West Palm Beach, FL, for powder production.

Pratt and Whitney attempted rapid solidification rate (RSR) atomization runs with the seven ingots. RSR powders were successfully produced from all the alloys with the exception of alloy 6 which apparently contained many ceramic particulates (possibly BeO) which clogged the 9.5-mm (0.375-in.) orifice of the crucible, thus terminating the melt flow.

Table 2 lists the melting temperatures (temperatures at which all solid pieces were visually observed to disappear), the pour temperatures, and the yields of –80-mesh powders of the six successful runs. The first run (alloy 1) was poured at a higher temperature as a safety factor to guarantee complete melting. Because this procedure was successful, the next four runs were run with a melt pour temperature of 1240–1320°C. The pour temperature of the final run was higher (1420°C) because of the higher melting point of TiAl.

Table 3 compares the Ti-Be alloy powder and ingot compositions with the target compositions, and also lists the O, C, N, and H concentrations. The Be concentrations in the initial charges were 30% higher than the desired final concentrations to compensate for possible loss during the two melting operations; however, there was no noticeable loss during casting or powder production. With the exception of Er_2O_3, all other additions were at acceptable levels. In alloy 8, the Er_2O_3 powder was sprinkled over the other chunks to attain a more homogeneous melt, but the cast ingot contained virtually no erbium. An alternate technique for adding erbium would be to enclose the Er_2O_3 powder in a titanium envelope and add this envelope to the other chunks before melting.

The levels of C, N, and H are acceptable, but the O level is high. The first alloy (#1) was cast at 1595°C and contained the highest concentration of oxygen. Although the alloys cast between 1425 and 1460°C contained less oxygen, no correlation exists between the casting temperatures and oxygen concentrations in these alloys. Probable sources of this oxygen pick-up are the relatively poor vacuum (40 Pa) during heating and the BeO wash used to protect the alumina crucible from the melt.

The elemental compositions of all of the powder lots were close to those of the starting ingots, and impurity concentrations did not increase during the production of this powder. The low C levels indicate that melt pouring occurred at a temperature sufficiently low to avoid reactions with the graphite crucible.

Table 2. The melting temperature, pour temperature and –80 mesh power yields of Ti-Al-Be powders produced by the RSR process.

Alloy	Melt temperature (°C)	Pour temperature (°C)	Yield (g)	% Yield
1	1370	1465	790	24.7
4	1170	1260	955	15.0
5	1200	1320	435	6.0
6	1130	1225	-	-
8	1150	1250	700	10.7
9	1160	1240	925	14.3
11	1325	1420	1905	28.7

89-224-301

Table 3. Compositions of Ti-Be Ingots and powders.

Alloy	Element	Ingot composition (wt %)	Powder composition (wt %)	Target composition (wt %)
1	Al	6.0	6.0	6
	V	3.0	2.8	4
	Be	3.8	3.9	2.75
	C	0.01	0.01	
	O	1.7	1.3	
	N	0.04	0.08	
	H	7 ppm	25 ppm	
4	Al	6.8	6.7	6
	V	5.0	4.5	4
	Be	7.3	7.3	5.5
	C	0.01	0.06	
	O	0.53	0.68	
	N	0.02	0.03	
	H	16 ppm	26 ppm	
5	Al	6.6	6.6	6
	V	4.2	3.8	4
	Be	6.9	7.1	5.5
	B	0.84	0.85	1
	Si	0.92	0.93	1
	C	0.76	0.79	1
	O	0.40	0.38	
	N	0.02	0.02	
	H	13 ppm	29 ppm	
6	Al	2.38		2.38
	V	22.5		26
	Be	3.98		2.75
	C	0.096		
	O	0.65		
	N	0.024		
	H	21 ppm		
8	Al	2.5	2.5	2.4
	V	25	27	26
	Be	4.0	4.0	2.75
	Er	0.1	0.1	2
	C	0.02	0.03	
	O	0.75	0.79	
	N	0.02	0.03	
	H	10 ppm	26 ppm	
9	Al	4.5	4.4	4.8
	V	24	27	26
	Be	6.7	7.2	5.5
	C	0.02	0.05	
	O	0.26	0 41	
	N	0.02	0.03	
	H	14 ppm	22 ppm	
11	Al	34	35	35
	Be	4.3	4.2	5
	C	0.02	0.18	
	O	0.07	0.14	
	N	0.02	0.02	
	H	12 ppm	23 ppm	

89-224-302b

4. CONSOLIDATION AND THERMOMECHANICAL PROCESSING OF RAPIDLY SOLIDIFIED Ti-Al-Be AND Ti-V-Be ALLOYS

RSR powders of the six Ti-Be alloys were extruded into rods by Nuclear Metals Incorporated, Concord, MA. The powders were canned in 50-mm-diameter mild steel cans with 3-mm-wall thickness, cold compacted at 280 MPa (40 ksi), evacuated at 400°C to 1 mPa (10^{-5} Torr), and sealed. The compacts were extruded in a 300-ton press through a 14.6 mm (0.575 in.) die to yield a reduction ratio of 12.6:1. It was necessary to extrude at the lowest possible temperature to avoid dispersoid coarsening and to impart maximum stored energy into the bar; a starting temperature of 950°C was chosen. All billets were heated in a nitrogen atmosphere for two hours. Billets 1A, 8A, 4A, and 9A were extruded in that order at 950°C. All billets extruded well enough to attempt to extrude at a lower temperature. Billets 1B, 8B, 4B, 9B, and 5A were then extruded in that order at 900°C. Billets 1B, 4B, and 5A experienced some can tearing approximately half way through the extrusion process; however, the affected regions were small and surfaces before and after the tears were sound. The can tearing is attributable to discontinuities in the cold compacts resulting from interruptions during the cold-compacting procedure, whereby two separate plugs of powder may have been formed.

When extrusion of billet 11A was attempted at 950°C, a stall occurred and no material flow was observed. Subsequent extrusions were attempted at 1000, 1100, and 1150°C and at a lower reduction ratio of 10.5:1, but no material flow was attained in any attempt. The billets of alloy 11 were then canned in 75-cm-diameter mild steel sleeves and extruded in a larger, 1400-ton, press. Successful extrusions were obtained at 1150°C with a reduction ratio of 14:1.

Photographs of the extrusions are shown in Figures 2a and b. Generally, 180 cm (5 feet) of good material was obtained for each extrusion. Two extrusions of each of alloys 1, 4, 8, and 9, one extrusion of alloy 5, and three extrusions of alloy 11 were produced.
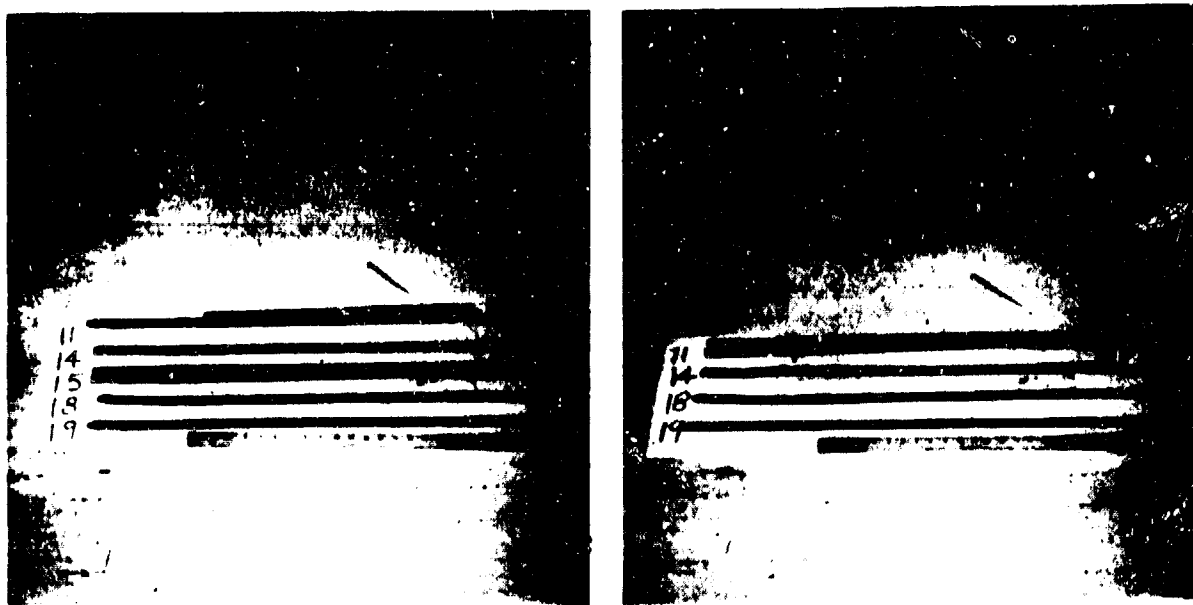
Figure 2. (a) Extrusions 1a, 4a, 5a, 8a, and 9a and
(b) extrusions 1b, 4b, 8b, and 9b.

5. MICROSTRUCTURES OF RAPIDLY SOLIDIFIED Ti–Al–Be AND Ti–V–Be ALLOYS

Ti-6Al-4V-4Be and Ti-25V-4Al-7Be were chosen as representative alloys and their microstructures were characterized by scanning electron microscopy (SEM), Auger electron spectroscopy (AES), and transmission electron microscopy (TEM). Figures 3a and b are scanning electron micrographs of a polished and etched Ti-6Al-4V-4Be sample. This alloy has a single-phase microstructure, in contrast to the two-phase microstructure of Ti-6Al-4V. Apparently, the b stabilizing effect of V is significantly reduced in the presence of Be. The 10-μm-diameter particles shown in Figure 3b have been identified as beryllium oxide by AES, as is indicated by the Auger spectrum in Figure 4. The composition (60-70 at.% Ti, 20-25 at.% Be, 8-12 at.% Al, and 2-4 at.% V) of the alloy determined from an AES spectrum of the matrix, shown in Figure 5, is in good agreement with chemical analysis. Figure 6 is a dark-field TEM micrograph showing the fine TiBe dispersion in the Ti-6Al-4V-7Be alloy.

89-224-289a

100 μm

100 μm
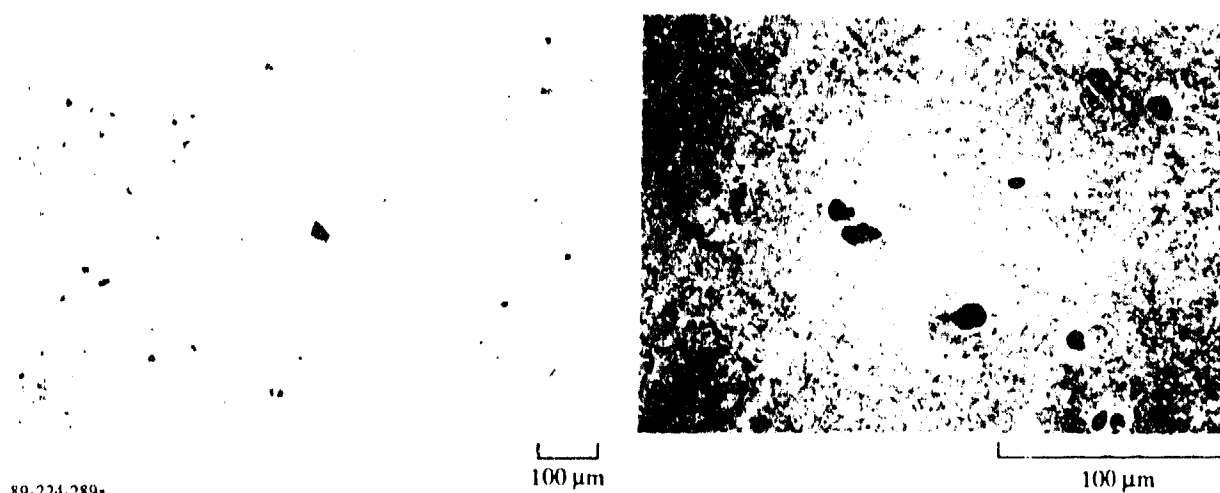
Figure 3. Scanning electron micrographs of the Ti-6Al-4V-4Be alloy showing the single-phase microstructure. Particles are beryllium oxide.

In contrast to the single-phase Ti-6Al-4V-4Be alloy, Ti-25V-4Al-7Be has the two-phase, fine-grained microstructure shown in Figure 7. The AES spectra shown in Figures 8 and 9 indicate the continuous phase to be Ti-35V-9Al (50-60 at.% Ti, 20-30 at.% V, and 7-10 at.% Al), and the discontinuous phase to be Ti-25Be-5V (50-60 at.% Be, 30-40 at.% Ti, and 3-5 at.% V). This alloy contains relatively large beryllium oxide particles as shown in Figure 10. The discontinuous phase contains fine dispersions of TiBe$_2$, as shown in Figures 11a and b.

11
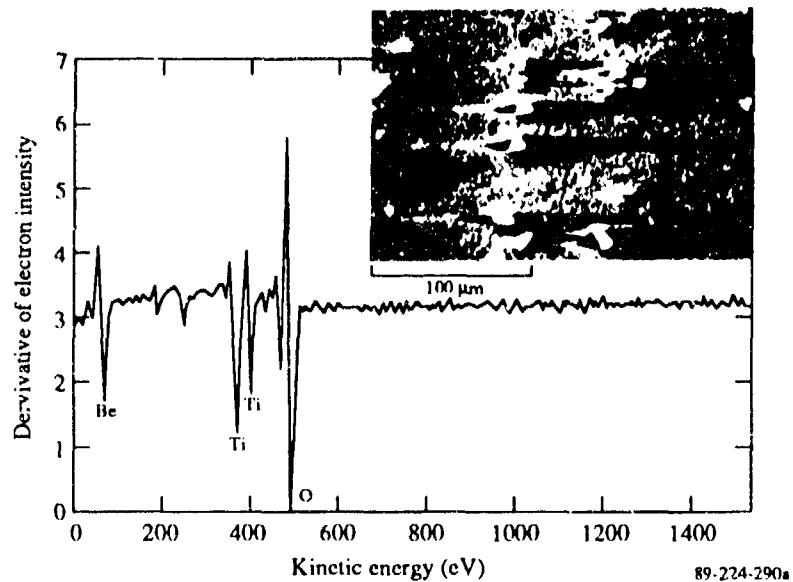
Figure 4. Auger electron spectroscopy (AES) spectrum which identifies the 10-μm-sized particles in the Ti-6Al-4V-4Be alloy to be beryllium oxide.
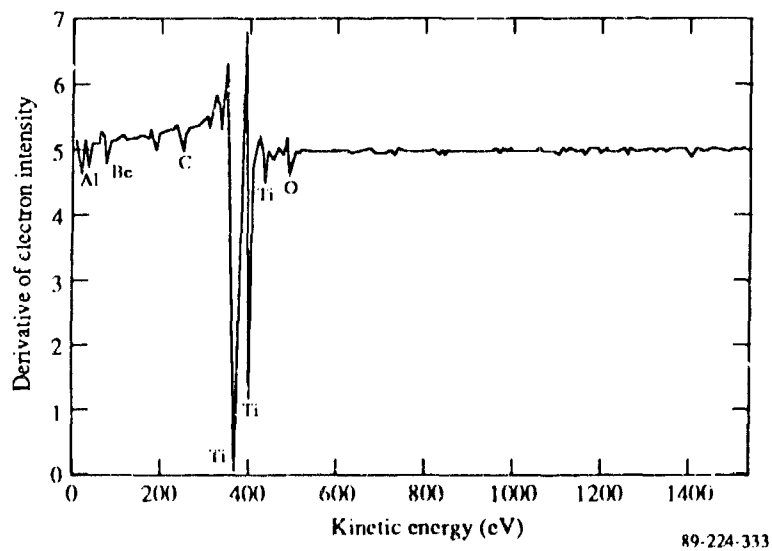
Figure 5. AES spectrum of the matrix of the Ti-6Al-4V-4Be alloy.

89-224-291

$\overline{}$
100 nm

Figure 6. Dark-field transmission electron micrograph (TEM)
showing the fine TiBe$_2$ dispersion in the Ti-6Al-4V-7Be alloy.
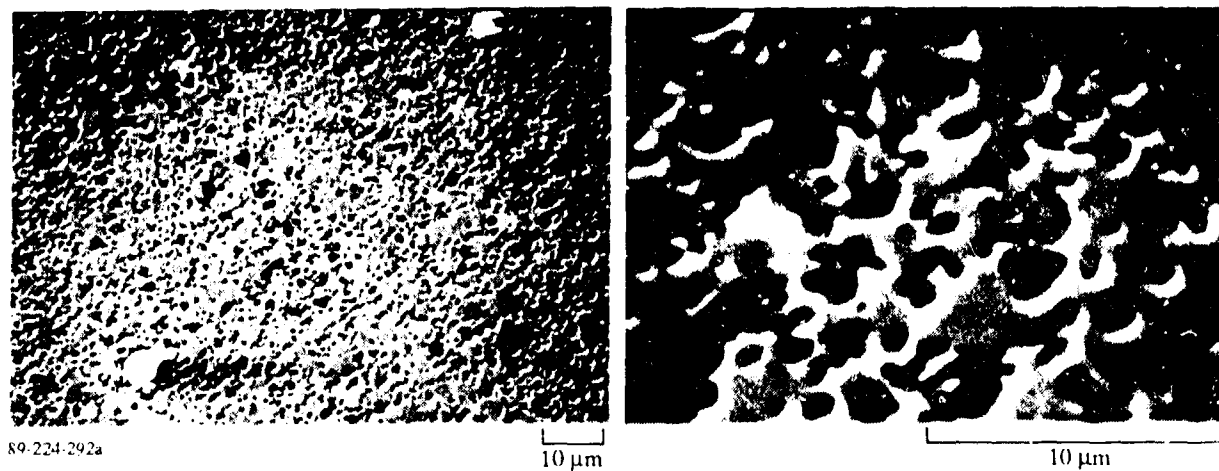
Figure 7. Scanning electron micrographs of the Ti-25V-4Al-7Be alloy, showing the two-phase, fine-grained microstructure.
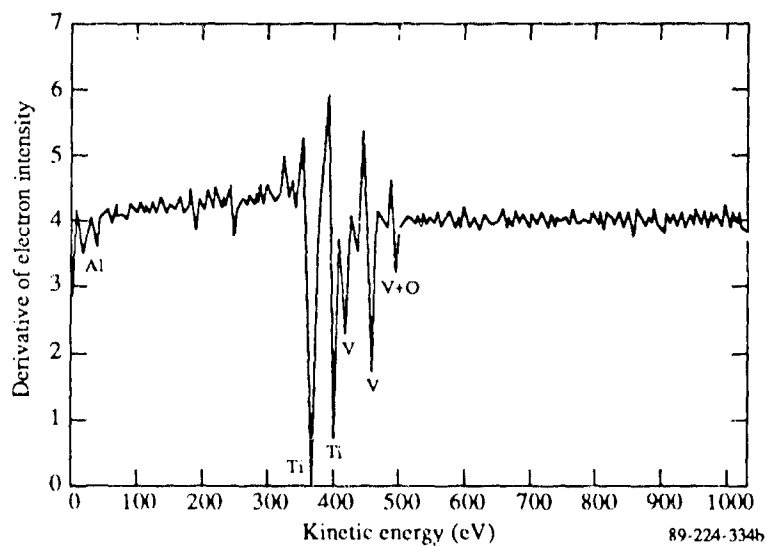
Figure 8. AES spectrum of the continuous phase of the Ti-25V-4Al-7Be alloy identifying it to be Ti-35V-9Al (50 - 60 at.% Ti, 30 - 40 at.% V, and 7 - 10 at.% Al).
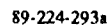
Figure 9. AES spectrum of the dark discontinuous phase of the Ti-25V-4Al-7Be alloy identifying it to be Ti-25Be-5V (50 - 60 at.% Be, 30 - 40 at.% Ti, and 3 - 5 at.% V).
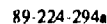
Figure 10. AES spectrum which identifies the 10-μm-sized particles in the Ti-25V-4Al-7Be alloy to be beryllium oxide.

89-224-295a

100 nm

200 nm
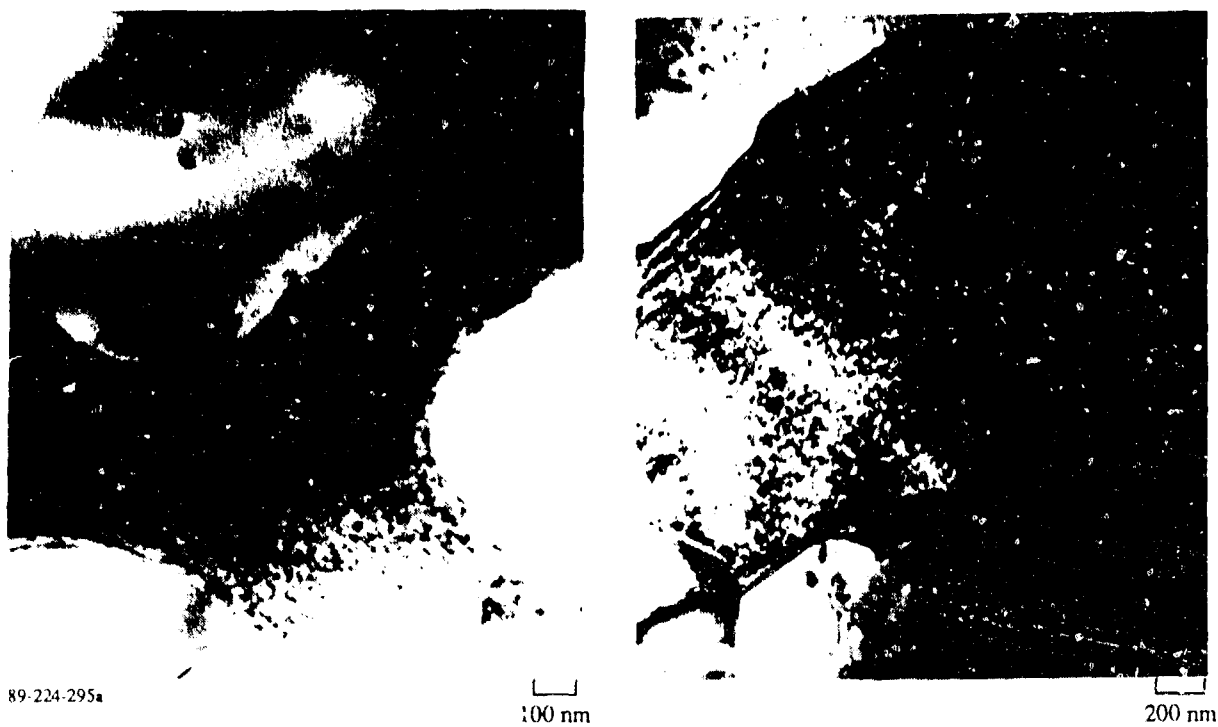
Figure 11. TEM micrograph showing the fine TiBe$_2$ dispersion in the Ti-25V-4Al-7Be alloy.

6. PHYSICAL AND MECHANICAL PROPERTIES OF RAPIDLY SOLIDIFIED Ti–Al–Be AND Ti–V–Be ALLOYS

6.1 Heat Treatments

Mechanical properties were determined for the six selected Ti–Be alloys in the as-extruded condition and after each of two heat-treatments. Specimens were sealed in evacuated quartz capsules for heat-treatments at 750°C for 96 h and 1000°C for 24 h to effect different degrees of grain coarsening.

6.2 Density of Ti–Be Alloys

The densities of selected alloy samples were determined by using the Archimedes technique with water at 23°C; these densities are compared with densities of the reference alloys in Table 4. Additions of 4 and 7 wt% Be to Ti–6Al–4V result in density decreases of 4.8 and 8.4%, respectively. Addition of 7 wt% Be to the β–alloy Ti–25V yields a density which is 3.4% less than Ti–6Al–4V and 11% less than a common β–alloy, Ti–15V–3Cr–3Al–3Sn. Addition of 4 wt% Be to the γ–titanium alloy Ti–35Al decreases its density by 4.6%, which is 19% lower than that of Ti–6Al–4V.

Table 4. Densities of reference alloy and Ti-Be alloy extrusions.

Alloy	Density (g/cm^3)	% reduction in density compared to reference alloy	% reduction in density compared to Ti-5Al-4V
Ti-6Al-4V	4.43		
Ti-6Al-4V-4Be	4.22	4.8	4.8
Ti-6Al-4V-7Be	4.06	8.4	8.4
Ti-15V-3Cr-3Al-3Sn	4.81		
Ti-25V-4Al-7Be	4.28	11	3.4
Ti-35Al-1.5V	3.76		
Ti-35Al-4Be	3.59	4.6	19

89-224-304b

6.3 Modulus of Ti–Be Alloys

The temperature dependence of the dynamic modulus of each class of alloys was determined by piezo-electric ultrasonic composite oscillation techniques (PUCOT). Addition of 7 wt% Be increases the modulus of Ti–6Al–4V (Reference 1) by at least 50% as shown in Figure 12; the modulus is approximately 25% greater than that of Ti–14Al–20Nb–3V–2Mo (Reference 2) and approaches the value of the γ–Ti alloy, Ti–35Al–1.5V (Reference 2).
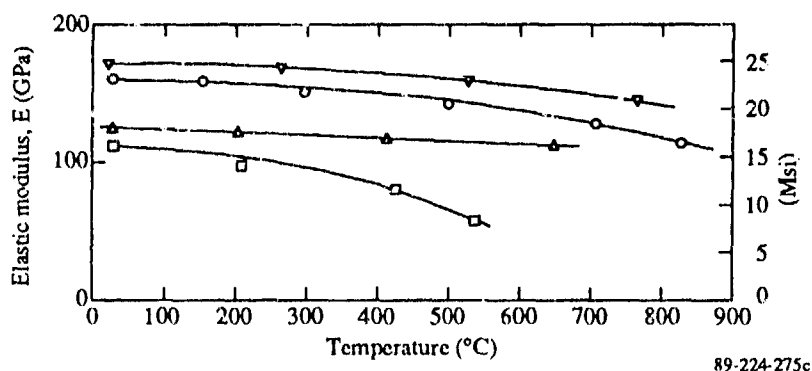
Figure 12. Temperature dependence of the dynamic modulus of
(o) Ti-6Al-4V-7Be, compared with published values of
(□) Ti-6Al-4V (Ref.1), (▲) Ti-14Al-20Nb-3V-2Mo (Ref.2), and (▼)
Ti-35Al-1.5V (Ref.2).

Addition of 7 wt% Be to Ti-25V results in a modulus which is 45% larger (Figure 13) than that of Ti-13V-11Cr-3Al (Reference 1), of a conventional β-alloy. Figure 14 shows that the modulus of Ti-35Al with 4 wt% Be is 15% larger than the modulus of Ti-35Al with 1.5 wt% V (Reference 2).
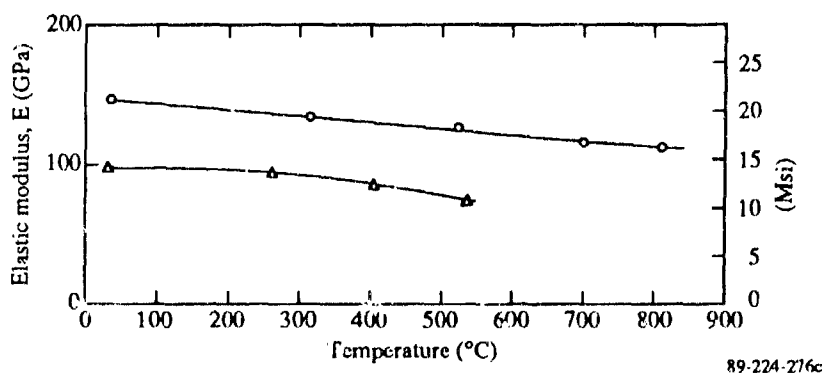
Figure 13. Temperature dependence of the dynamic modulus of (o) Ti-25V-7Be compared with published values of (▲) Ti-13V-11Cr-3Al (Ref.1).
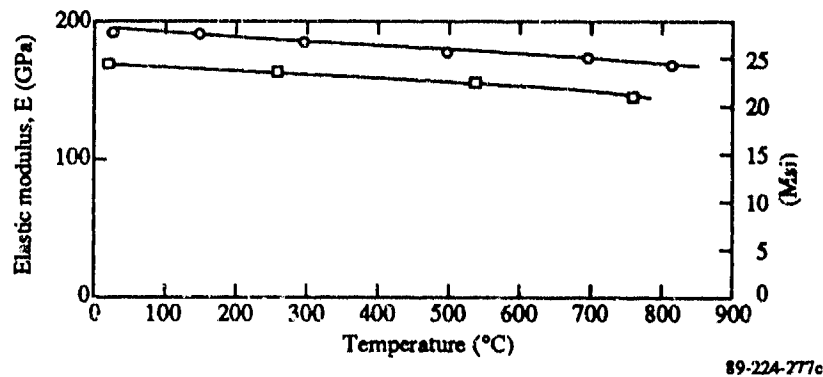
Figure 14. Temperature dependence of the dynamic
modulus of (o) Ti-35Al-4Be compared with published
values of (□) Ti-35Al-1.5V (Ref.2).

6.4 Elevated-Temperature Tensile and Compressive Strengths

Elevated-temperature tensile and compression tests were performed in air with a hydraulically actuated, servoloop-controlled, test system (MTS Series 810) and a three-zone resistance-heated furnace (Applied Test Systems model 2961). Figure 15a shows the circular-cross-section tensile specimen geometry. Button-head grips and water-cooled pull-rods linked the specimen to the load cell and actuator. The compression specimen geometry is shown in Figure 15b. Both tensile and compression specimens were fabricated with conventional machining techniques employing tungsten-carbide-tipped cutters. For the higher-temperature tests, forces were imparted to the compression specimens through Inconel 625 inserts sandwiched between compression rams; deformation of the inserts was negligible. Tool-steel inserts were used for 25°C compression testing. Unless otherwise noted, strain rates were 5×10^{-4}/s and 5×10^{-3}/s for tension and compression testing, respectively.
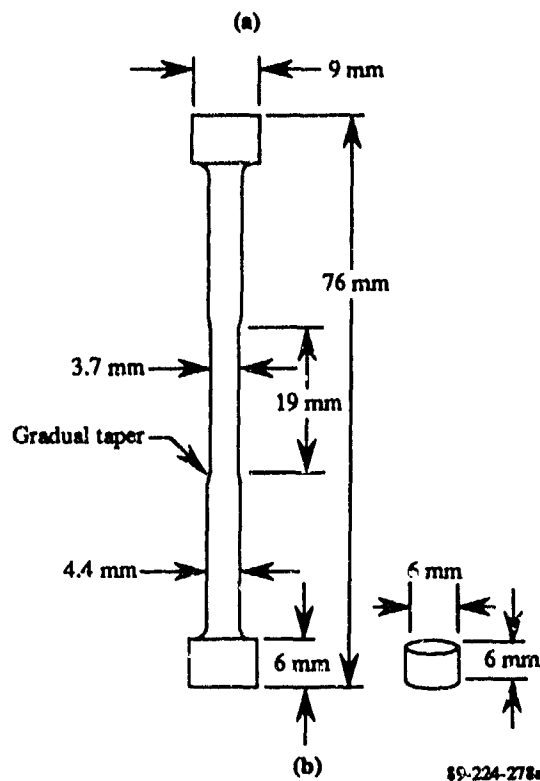
Figure 15. (a) Tensile specimen geometry and
(b) compression specimen geometry.

The influence of heat treatments on compressive strengths of Ti-6Al-4V-4Be alloy are shown in Figure
16. The 1000°C/24-h treatment yielded consistently higher strengths than the 750°C/100-h treatment. The
flow stresses are significantly higher in heat treated alloys than in extruded alloys. Tension and compression
strength values at 25-815°C are listed in Tables 5-10. The tensile specimens exhibited no plastic strain at
25°C. This room temperature brittleness is attributed to the high oxygen concentrations in the alloys. In
the as-extruded condition, the brittle/ductile transition occurred between 500 and 600°C for
Ti-24V-4Al-7Be and Ti-6Al-4V-4Be, and between 600 and 700°C for Ti-6Al-4V-7Be. The brittle/ductile
transition temperature was higher in the heat treated alloys. The extrusion temperature of the bars had no
significant effect on properties. The specific strengths (density normalized strength values) are listed in
Tables 11-16.

The Be levels do not significantly affect the mechanical properties in the as-extruded condition. Howev-
er, after each of the heat-treatments, the alloys containing 7 wt% Be are considerably (20-60%) stronger
than the comparable alloys which contain only 4 wt% Be.

Alloy 5, containing small amounts of B, C, and Si, was more brittle than alloy 4 as evidenced by the shat-
tering of the specimens before yielding during room temperature compression testing (Table 8). However,
this alloy has high strengths at 600 and 700°C (Tables 8-10).

20
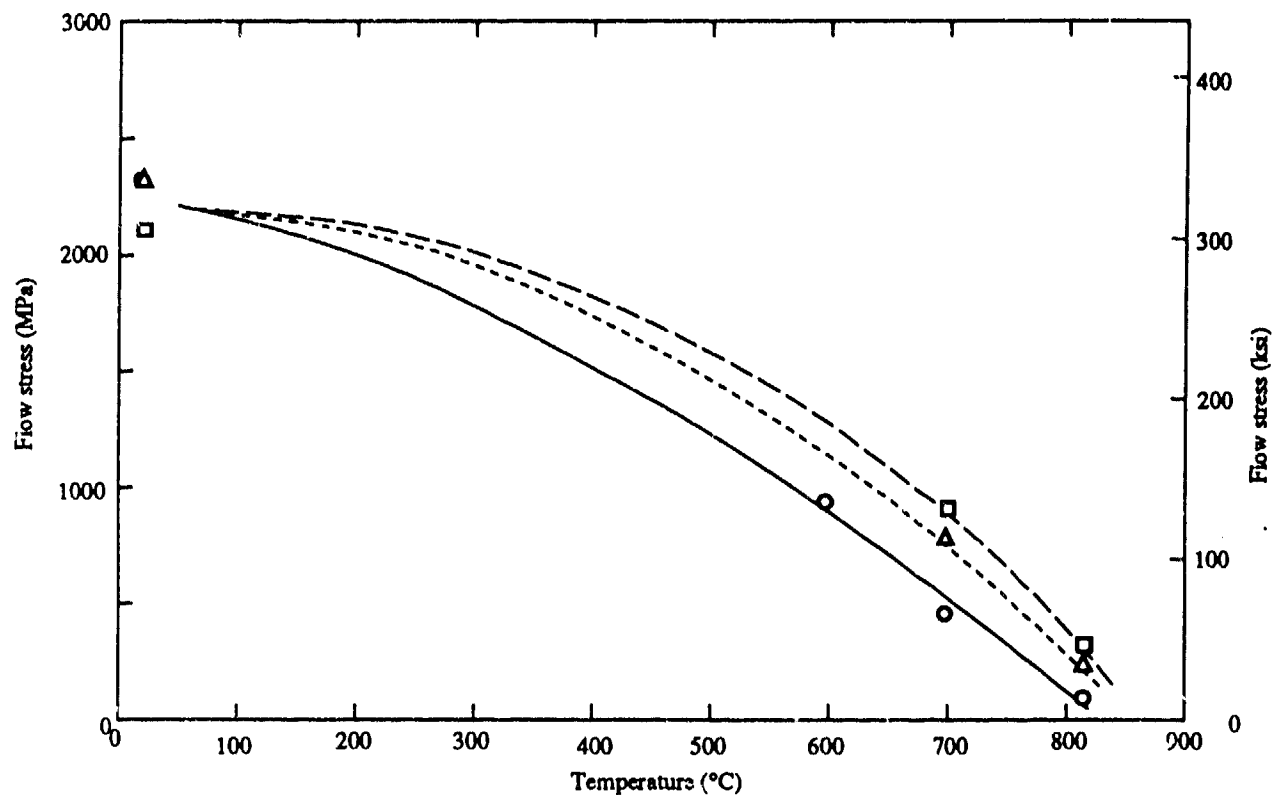
Figure 16. Temperature dependence of the compressive flow stress of Ti-6Al-4V-4Be, (○) as-extruded, (Δ) following a 750°C/100 h heat treatment, and (□) following a 1000°C/24 h heat treatment.

Table 5. Elevated temperature tensile fracture, yield, and ultimate stresses and total elongations of Ti-Al-Be alloys in the as-extruded condition.

Alloy	Extrusion temperature (°C)	Test temperature								
		25° C	400° C	500° C	600° C			700° C		
		FS MPa (ksi)	FS MPa (ksi)	FS MPa (ksi)	YS MPa (ksi)	UTS MPa (ksi)	Elong (%)	YS MPa (ksi)	UTS MPa (ksi)	Elong (%)
Ti-6Al-4V-4Be	950	675 (98.2)			990 (144)	1065 (155)	.7	545 (79.0)	575 (83.1)	5.7
Ti-6Al-4V-7Be	950	680 (98.6)			760* (110)			545 (79.2)	600 (86.9)	5.7
	900	625 (90.8)			865* (126)					
Ti-24V-4Al-7Be	950	1000 (145)	1085 (157)		875 (127)	920 (134)	6.5			
	900	1190 (173)		1075 (156)						

$\dot{\varepsilon} = 5 \times 10^{-4}/s$

YS - yield stress
UTS - ultimate tensile stress
FS,* - fracture stress

89-224-305c

Table 6. Elevated temperature tensile fracture, yield, and ultimate stresses and total elongations of Ti-Al-Be alloys following a 750°C/94 h/AC heat treatment.

Alloy	Extrusion temperature	Test temperature			
		815° C			
		YS MPa (ksi)	UTS MPa (ksi)	Elong (%)	$\dot{\varepsilon}$
Ti-6Al-4V-7Be	950	149 (21.7)	156 (22.6)	> 40	5×10^{-4}
		201 (29.1)	209 (30.3)	> 40	10^{-3}
Ti-24V-4Al-7Be	950	105 (15.2)	112 (16.3)	> 40	5×10^{-4}
		134 (19.5)	144 (20.9)	> 40	10^{-3}

YS - yield stress
UTS - ultimate tensile stress

89-224-306d

Table 7. Elevated temperature tensile fracture, yield, and ultimate stresses and total elongations of Ti-Al-Be alloys following a 1000°C/24 h/AC heat treatment.

Alloy	Extrusion temperature	Test temperature						
		700° C			815° C			
		YS MPa (ksi)	UTS MPa (ksi)	Elong (%)	YS MPa (ksi)	UTS MPa (ksi)	Elong (%)	$\dot{\varepsilon}$
Ti-6Al-4V-7Be	950	414 (60.0)*			296 (43.0)	325 (46.8)	5.7	5×10^{-4}
					287 (41.6)	325 (47.1)	4.7	5×10^{-4}
					397 (57.6)	432 (62.7)	5.7	10^{-3}
Ti-24V-4Al-7Be	950	305 (44.4)	352 (51.1)	11	148 (21.4)	154 (22.3)	35	5×10^{-4}
					141 (20.5)	160 (23.4)	27	5×10^{-4}
					190 (27.4)	197 (28.5)	35	10^{-3}

YS - yield stress
UTS - ultimate tensile stress
* - fracture stress

89-224-307d

Table 8. Elevated temperature compressive flow stresses of Ti-Al-Be alloys in the as extruded condition.

Alloy	Extrusion temperature (° C)	Flow stress MPa (ksi)				
		Test temperature				
		25° C	600° C	700° C	815° C	982° C
Ti-6Al-4V-4Be	950	2250 (326) 2345 (340)	935 (135)	460 (66.8)	100 (14.7)	
	900	2480 (359)	1255 (182)	650 (94.5)	125 (18.5)	
Ti-6Al-4V-7Be	950	2000 (290)	1130 (164)	545 (79.4)	130 (18.6)	
	900	2225 (323)	980 (142)	555 (80.8)	65 (9.5)	
Ti-6Al-4V-7Be-1B-1C-1Si	900	1480 (215)	1620 (235)	850 (123)	80 (11.4)	
Ti-24V-2.5Al-4Be	950	1260 (183)	564 (81.8)	240 (34.6)	70 (10.1)	
	900	1305 (189)	570 (82.5)	218 (31.6)	65 (9.6)	
Ti-24V-4Al-7Be	950	1630 (236) 1725 (250)	540 (78.2)	225 (32.9)	55 (8.1)	
	900	1780 (258)	780 (113)	335 (48.7)	85 (12.0)	
Ti-35Al-4Be	1150	1340 (194)		1490 (216)	1080 (157)	280 (40.7)
Ti-6Al-4V		975 (142)	470 (68)	285 (41.6)		

$\dot{\varepsilon} = 10^{-3}/s$

89-0224-308c

Table 9. Elevated temperature compressive flow stresses of Ti-Al-Be alloys following a 750°C/94h/AC heat treatment.

Alloy	Extrusion temperature (°C)	Flow stress MPa (ksi)		
		Test temperature		
		25°C	700°C	815°C
Ti-6Al-4V-4Be	950	2300(335)		235(34.0)
	900		765(111)	180(26.3)
Ti-6Al-4V-7Be	950		960(139)	398(57.8)
	900		975(142)	296(43.0)
Ti-6Al-4V-5Be-1B-1C-1Si	900		1285(186)	230(33.4)
Ti-24V-2.5Al-4Be	950	1290(187)		
	900		300(43.6)	
Ti-24V-4Al-7Be	950		425(61.4)	130(19.2)
	900		455(65.8)	125(17.9)

$\dot{\epsilon} = 10^{-3}/s$

89-224-309c

Table 10. Elevated temperature compressive flow stresses of Ti-Al-Be alloys following a 1000°C/24h/AC heat treatment.

Alloy	Extrusion temperature (°C)	Flow stress MPa (ksi)		
		Test temperature		
		25°C	700°C	815°C
Ti-6Al-4V-4Be	950	2100(305)	885(128)	
	900	2110(306)		320(46.4)
Ti-6Al-4V-7Be	950		1010(146)	{425(61.5), 405(59.0)}
	900		990(143)	405(58.6)
Ti-6Al-4V-5Be-1B-1C-1Si	900		1195(173)	300(43.5)
Ti-24V-2.5Al-4Be	950	1390(202)	345(49.7)	
	900		265(38.1)	145(20.9)
Ti-24V-4Al-7Be	950		440(63.9)	{200(29.3), 170(24.8)}
	900		430(62.2)	176(25.5)

$\dot{\epsilon} = 10^{-3}/s$

89-224-310c

Table 11. Elevated temperature tensile specific strengths of Ti-Al-Be alloys in the as-extruded condition.

Alloy	Extrusion temperature	Test temperature								
		25° C	400° C	500° C	600° C			700° C		
		$\frac{FS\ MPa}{g/cm^3}$	$\frac{FS\ MPa}{g/cm^3}$	$\frac{FS\ MPa}{g/cm^3}$	$\frac{YS\ MPa}{g/cm^3}$	$\frac{UTS\ MPa}{g/cm^3}$	Elong (%)	$\frac{YS\ MPa}{g/cm^3}$	$\frac{UTS\ MPa}{g/cm^3}$	Elong (%)
Ti-6Al-4V-4Be	950	160			235	252	.7	129	136	5.7
Ti-6Al-4V-7Be	950	167			187*			134	148	5.7
	900	154			213*					
Ti-24V-4Al-7Be	950	234	253		214	225	6.5			
	900	288		251						

$\varepsilon = 5 \times 10^{-4}$/s

YS - specific yield stress
UTS - specific ultimate stress
FS, * - specific fracture stress

89-0224-311d

Table 12. Elevated temperature tensile specific strengths of Ti-Al-Be alloys following a 750° C/94 h/AC heat treatment.

Alloy	Extrusion temperature (°C)	Test temperature			
		815° C			
		$\frac{YS\ MPa}{g/cm^3}$	$\frac{UTS\ MPa}{g/cm^3}$	Elong (%)	$\dot{\varepsilon}$
Ti-6Al-4V-7Be	950	37	38	>40	5×10^{-4}
		50	51	>40	10^{-3}
Ti-24V-4Al-7Be	950	25	26	>40	5×10^{-4}
		31	34	>40	10^{-3}

YS - yield stress
UTS - ultimate tensile stress

89-0224 312d

Table 13. Elevated temperature tensile specific strengths of Ti-Al-Be alloys following a 1000°C/24 h/AC heat treatment.

Alloy	Extrusion temperature (°C)	Test temperature						
		700° C			815° C			
		$\frac{YS\ MPa}{g/cm^3}$	$\frac{UTS\ MPa}{g/cm^3}$	Elong (%)	$\frac{YS\ MPa}{g/cm^3}$	$\frac{UTS\ MPa}{g/cm^3}$	Elong (%)	$\dot{\varepsilon}$
Ti-6Al-4V-7Be	950	102*			73	80	5.7	5×10^{-4}
					71	80	4.7	5×10^{-4}
					98	106	5.7	10^{-3}
Ti-24V-4Al-7Be	950	71	82	11	34	36	35	5×10^{-4}
					23	37	27	5×10^{-4}
					44	46	35	10^{-3}

YS - specific yield stress
UTS - specific ultimate stress
* - specific fracture stress

89-0224-313d

Table 14. Elevated temperature compressive specific strengths of Ti Al Be alloys in the as extruded condition.

Alloy	Extrusion temperature (° C)	Specific strength $\frac{MPa}{g/cm^3}$				
		Test temperature				
		25° C	600° C	700° C	815° C	982° C
Ti-6Al-4V-4Be	950	{ 533 556 }	222	109	24	
	900	588	297	154	30	
Ti-6Al-4V-7Be	950	493	278	134	32	
	900	548	241	137	16	
Ti-24V-2.5Al-4Be	950	286	128	55	16	
	900	297	130	50	15	
Ti-24V-4Al-7Be	950	{ 381 403 }	126	53	13	
	900	416	182	78	20	
Ti-35Al-4Be	1150	373		415	301	78
Ti-6Al-4V		220	106	64		

$\dot{\varepsilon} = 10^{-3}$/s

89-224-314b

Table 15. Temperature dependence of compressive specific strength
of Ti-Al-Be alloys following a 750°C/94 h/AC heat treatment.

Alloy	Extrusion temperature	Specific strength $\frac{MPa}{g/cm^3}$		
		Test temperature		
		25°	700° C	815° C
Ti-6Al-4V-4Be	950	545		56
	900		181	43
Ti-6Al-4V-7Be	950		236	98
	900		240	73
Ti-24V-2.5Al-4Be	950	293		
	900		68	
Ti-24V-4Al-7Be	950		99	30
	900		106	29

$\dot{\varepsilon} = 10^{-3}/s$

89-224-315c

Table 16. Temperature dependence of compressive specific strength of
Ti-Al-Be alloys following a 1000°C/94 h/AC heat treatment.

Alloy	Extrusion temperature	Specific strength $\frac{MPa}{g/cm^3}$		
		Test temperature		
		25°	700° C	815° C
Ti-6Al-4V-4Be	950	498	210	
	900	500		76
Ti-6Al-4V-7Be	950		248	102
	900		244	100
Ti-24V-2.5Al-4Be	950	316	78	
	900		60	33
Ti-24V-4Al-7Be	950		103	$\{^{47}_{40}\}$
	900		100	41

$\dot{\varepsilon} = 10^{-3}/s$

89-224-316c

Figure 17 compares the temperature dependence of the specific compressive strength of Ti-6Al-4V-7Be (1000°C/24-h anneal) with Ti-6Al-4V (Reference 1). The strengths are more than doubled by the Be addition over the entire temperature range. Figure 18 compares the specific tensile strengths of Ti-6Al-4V-7Be and Ti-6Al-4V (Reference 1). The specific tensile strength of Ti-6Al-4V-7Be at 25°C is low because the sample failed before yielding, and the dotted line shows the anticipated strengths had the sample not fractured before yielding. Figures 19 and 20 compare the specific tensile and compressive strengths, respectively, of Ti-24V-4Al-7Be with Ti-15V-3Cr-3Al-3Sn (Reference 3) as functions of temperature. The tensile specimens fractured before yield at 25, 400, and 500°C. However, the Be-containing alloys have considerably higher values of specific strength.

89-224-280d
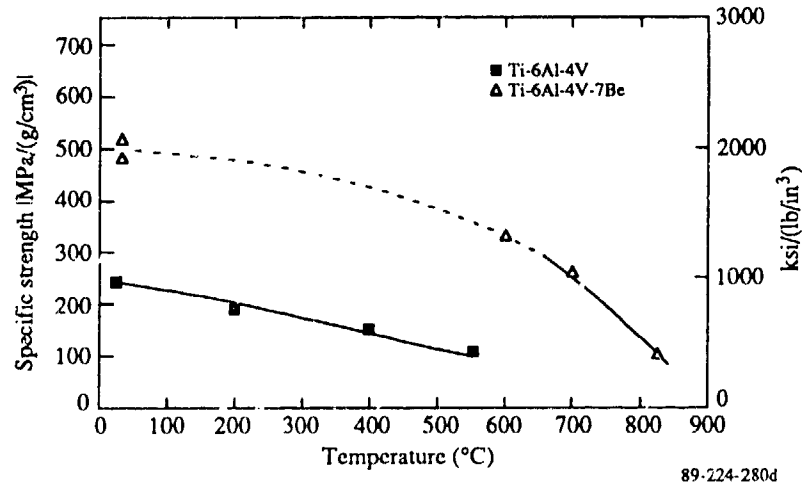
Figure 17. Temperature dependence of compressive specific strength of (Δ) Ti-6Al-4V-7Be compared with published values of (■) Ti-6Al-4V (Ref.1).

89-224-281c
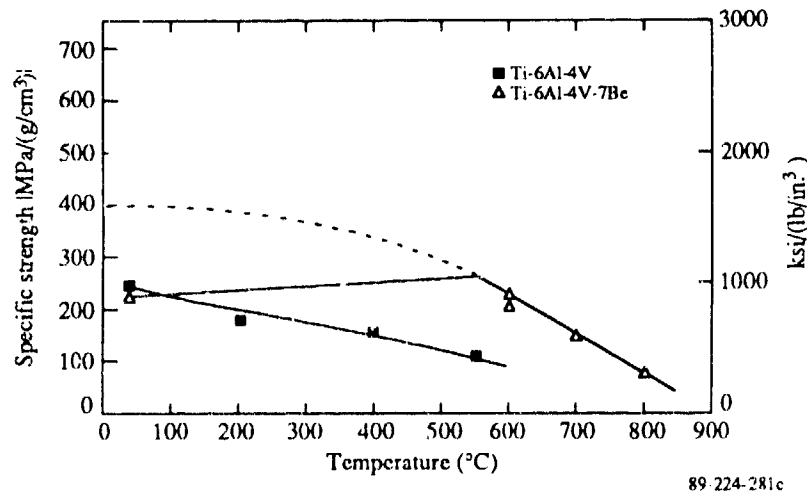
Figure 18. Temperature dependence of tensile specific strength of (Δ) Ti-6Al-4V-7Be compared with published values of (■) Ti-6Al-4V (Ref.1).
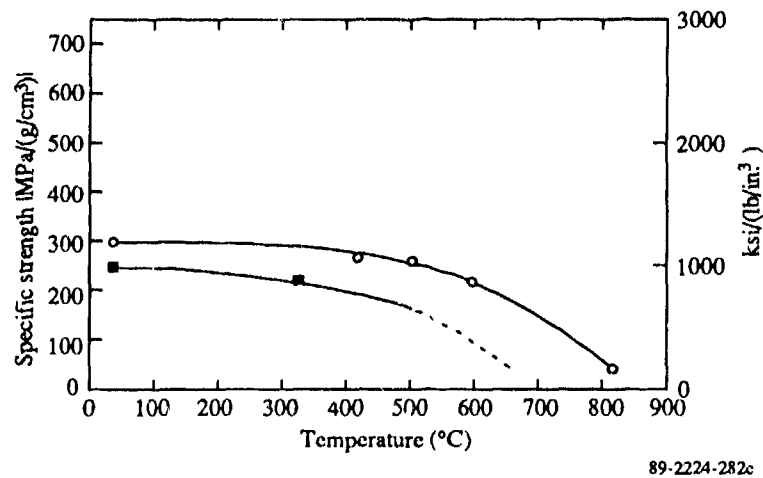
Figure 19. Temperature dependence of tensile specific strength of (o) Ti-25V-4Al-7Be compared with with published values of (■) Ti-15V-3Cr-3Al-3Sn (Ref.3).
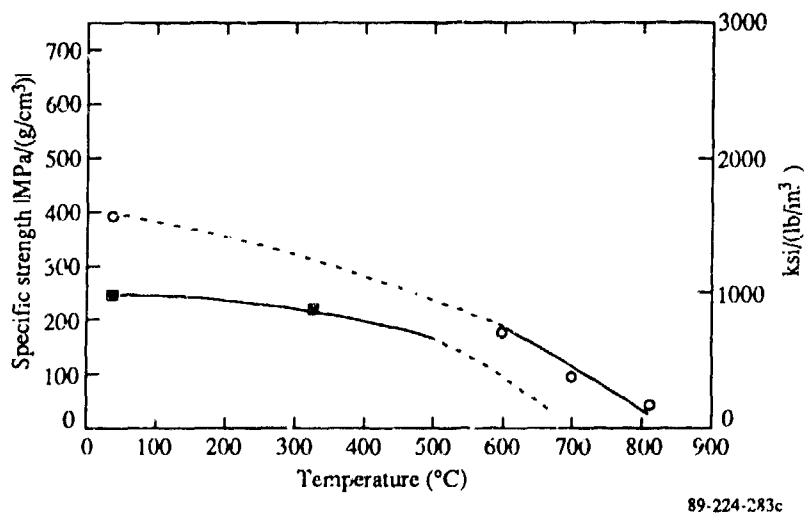
Figure 20. Temperature dependence of compressive specific strength of (o) Ti-25V-4Al-7Be compared with published values of (■) Ti-15V-3Cr-3Al-3Sn (Ref.3).

Figure 21 compares the compressive specific strengths of Ti-6Al-4V-7Be and Ti-34Al-4Be alloys with those of gamma (Reference 2) and alpha-2 (Reference 2) titanium aluminides and conventional titanium alloys (Reference 1). At temperatures below 800°C, the Ti-6Al-4V-7Be alloy has significantly higher strength than the titanium aluminides. The limited data for Ti-34Al-4Be show it to be very strong above 700°C; however, the alloy is brittle.
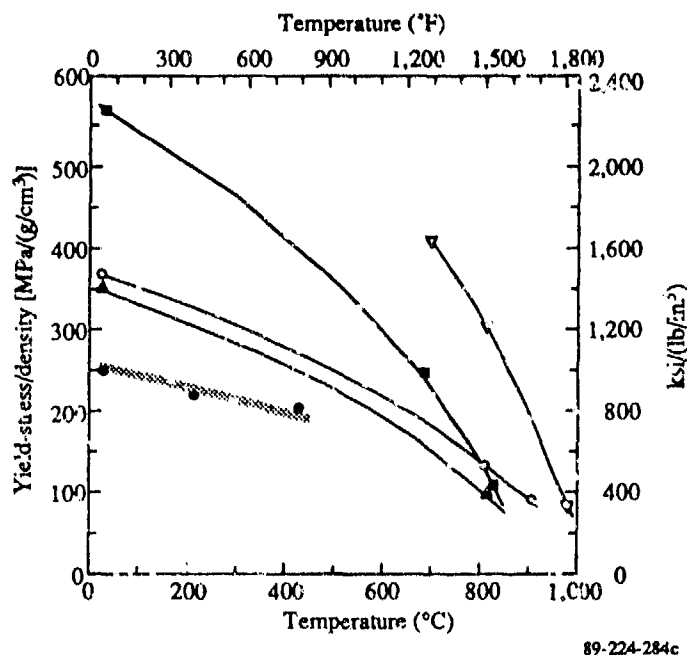
Figure 21. Temperature dependence of compressive specific strength of
(■) Ti-6Al-4V-7Be and (v) Ti-34Al-4Be compared with published values
for (•) Ti-6Al-4V (Ref.1), (▲) Ti₃Al base alloys (Ref.2), and (○) TiAl
base alloys (Ref.?).

6.5 Creep Properties

Creep properties of Ti-25V-4Al-7Be and Ti-6Al-4V-7Be were determined at 700°C by compression
testing using the specimen geometry shown in Figure 15b. The stress dependence of the creep rates for all
three heat-treated conditions of Ti-25V-4Al-7Be are compared with published values of Ti-6Al-4V (Reference 4) and Ti-6Al-2Sn-4Zr-2Mo (Reference 4) in Figure 22. The 1000°C/24-h annealed Ti-25V-4Al-7Be
has an order-of-magnitude better creep resistance than Ti-6Al-2Sn-4Zr-2Mo. This result is particularly
noteworthy because beta alloys in general have poor creep resistance. All three heat-treated conditions of
Ti-25V-4Al-7Be are much superior to Ti-6Al-4V.

Figure 23 shows that the creep rates are significantly lower in Ti-6Al-4V- 7Be than in
Ti-6Al-2Sn-4Zr-2Mo (Reference 4) and Ti-6Al-4V (Reference 4).
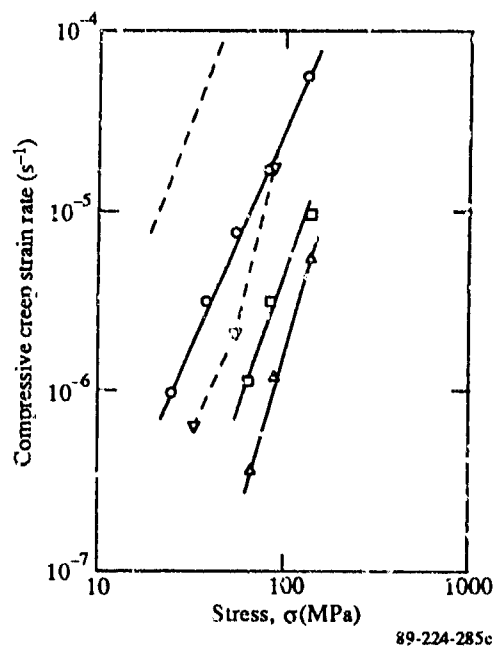
Figure 22. Stress dependence of creep rates at 700°C of Ti-25V-4Al-7Be, (o) as-extruded, and after (□) 750°C/96 h and (▲) 1000°C/24 h heat treatment, compared with published values for (▽) Ti-6Al-2Sn-4Zr-2Mo (Ref.4) and (- -) Ti-6Al-4V (Ref.4).
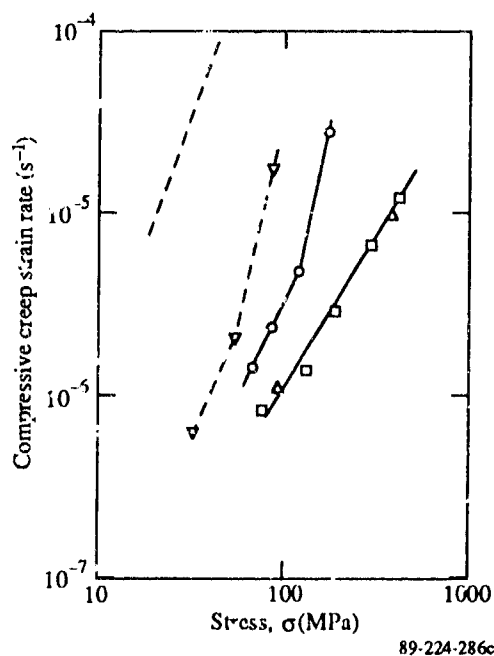
Figure 23. Stress dependence of creep rates at 700°C of Ti-6Al-4V-7Be, (o) as-extruded, and after (□) 750°C/96 h and (▲) 1000°C/24 h heat treatment, compared with published values for (▽) Ti-6Al-2Sn-4Zr-2Mo (Ref.4) and (- -) Ti-6Al-4V (Ref.4).

6.6 Fracture Toughness

The specimen geometry shown in Figure 24 was used for fracture toughness determinations. The specimens were fabricated by electrical discharge machining and were notched with a 0.1-mm- (0.004-in.) diameter wire. Testing was in accordance with ASTM E399. Stable cracks were initiated by subjecting the specimens to axial compressive fatigue loading. The fracture toughness values of two specimens of Ti-25V-4Al-7Be along with those of Ti-6Al-4V (Reference 5) and titanium aluminides are listed (Reference 2) in Table 17. Although the values for Ti-25V-4Al-7Be are considerably less than the values for Ti-6Al-4V, they compare favorably with the titanium aluminides. The values of the Ti-Be alloy might have been greater had the oxygen concentration been lower. The fracture surface of the Ti-25V-4Al-7Be specimen (Figure 25) shows ductile-dimple fracture.
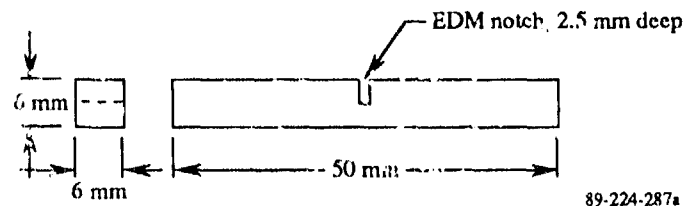
Figure 24 Fracture toughness specimen geometry.

Table 17. Fracture toughness values of two
Ti-25V-4Al-7Be samples compared with published
values for other alloys.

	MPa$\sqrt{m}$
Ti-25V-4Al-7Be	18.4 19.1
Ti-6Al-4V (Ref 5)	45
TiAl based alloys (Ref 2)	10
Ti$_3$Al based alloys (Ref 2)	15

89-224-317a

87-224-288a

10 µm

100 µm
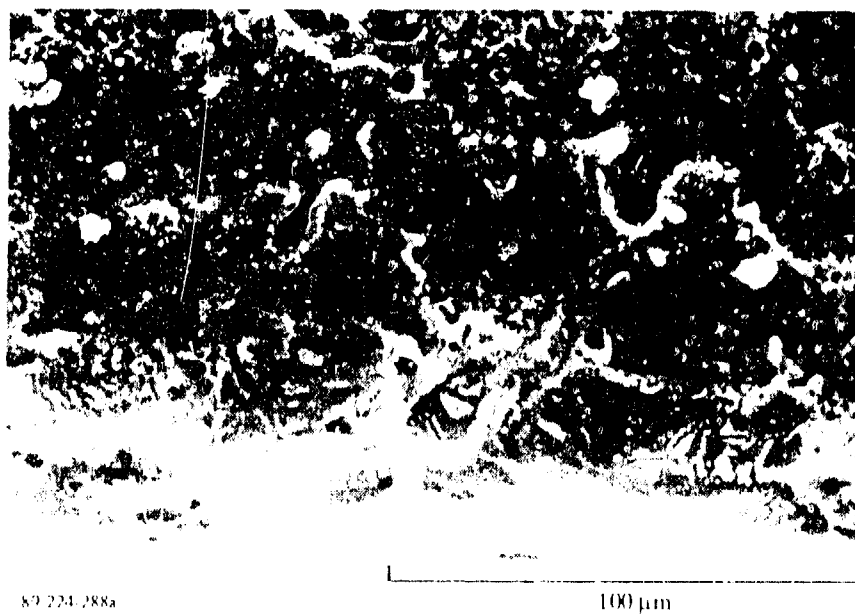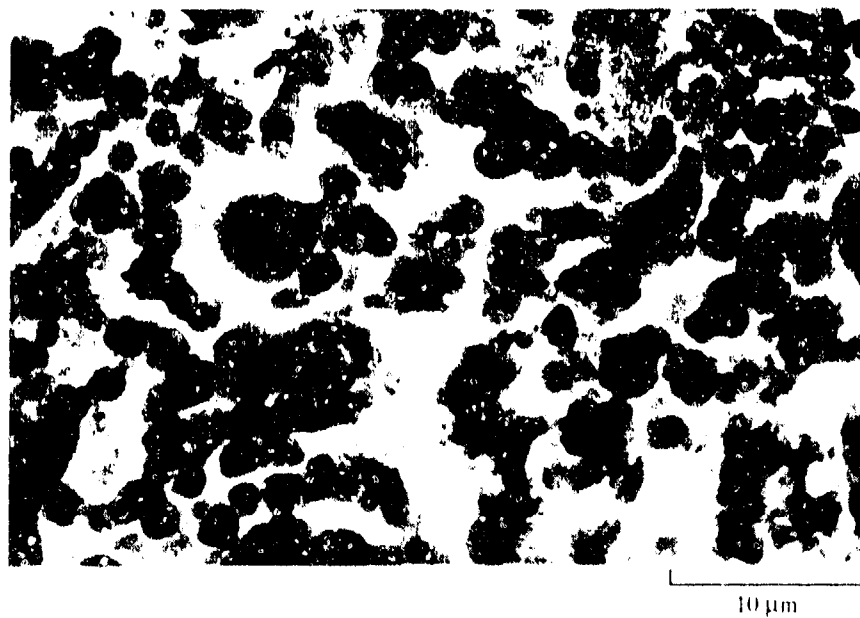
Figure 25. Scanning electron micrographs showing
ductile-dimple fracture surfaces of Ti-25V-4Al-7Be
fracture toughness specimen.

7. Ti–Al–Mg AND Ti–Al–Li ALLOY DEVELOPMENT

Although the use of Li and Mg as alloying elements in Ti can effect large reductions in density, standard methods of preparation are not feasible because of the volatility of Li and Mg at the Ti melting temperature. A secondary thrust of the program on Development of Lightweight Titanium Alloys was to investigate different techniques of producing Ti–Al–Li and Ti–Al–Mg alloys. The techniques investigated and the results obtained are described below.

7.1 Powder Production by Laser–Melting/Spin–Atomization

Compacts of the 8 alloys listed in Table 18 were produced by blending elemental powders, filling the powders in 25–mm– (1–in.) diameter Ti cans, vacuum outgassing and sealing, and hot isostatic pressing (HIPing) at 210 MPa. Samples HIPed at 800°C were not fully compacted and Li was observed to bubble in cooling water during subsequent machining. HIPing at 1000°C produced fully consolidated compacts. The Ti can was removed and conversion of compacts to powder was attempted by a laser–melting spin–atomization method. The compacts were mounted on a high-speed motor, rotated at 28 000 rpm in an argon environment, and hit with short bursts of radiation from a 12 kW CO_2 laser to maintain a molten layer on the tip (Figure 26). Centrifugal force caused the expulsion of fine droplets which were rapidly solidified. The details of the experimental procedure are described in Reference 6. Laser power time duration, and beam location were varied to obtain yields of fine powders. Generally, 5–s durations of a slightly off–center 6–kW beam yielded the best results. Yields of –60–mesh powder were small, about 2–5 g. Powders of three of the alloys were chemically analyzed and the results are shown in Table 19. Significant amounts of Li and Mg were lost during powder production despite the short lifetime of the molten layer before atomization. All three alloys contain excessively high levels of oxygen, nitrogen, hydrogen, and carbon.

Table 18. Ti-Li and Ti-Mg based alloys selected for laser-melting/spin-atomization (LAMSA) study.

A	Ti-8Al-2Li
B	Ti-8Al-1Li-3Mg-1B-1C-1Si
C	Ti-26V-5Mg-3Li-1Al
D	Ti-26V-3Al-3Mg-1B-1C-1Li
E	PREP (Ti-6Al-4V) + 10% (Al-20Li)
F	PREP (Ti-V-Cr) + 20% (Al-20Li)
G	PREP (Ti-6Al-4V) + 5% Mg
H	PREP (Ti-V-Cr) + 5% Mg

89-224-318a
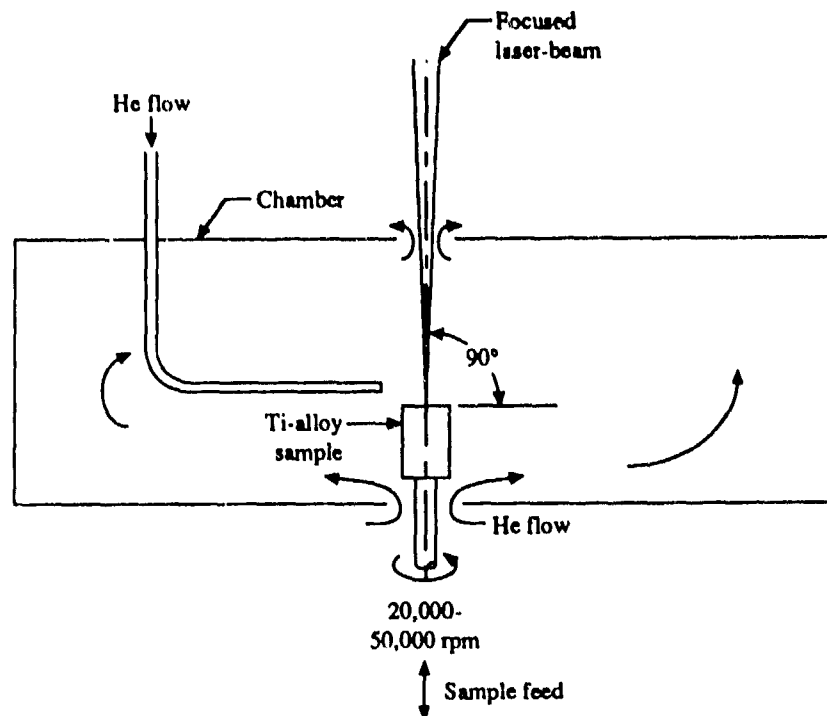
89-224-432

Figure 26. Experimental arrangement for production of rapidly
solidified titanium-alloy powders laser melting/spin atomization
(LAMSA).

Table 19. Compositions in weight percent of powders produced by LMSA.
target compositions are shown for comparison.

Alloying element	Alloy C		Alloy E		Alloy H	
	Target composition weight %	Actual composition weight %	Target composition weight %	Actual composition weight %	Target composition weight %	Actual composition weight %
Al	6	6.85	13	13.5		
V	26	24.4	4	5.34	24	30.7
Cr					10	13.8
Mg	5	1.53			5	2.47
Li	3	0.59	2	0.78		
O		9.87		4.66		1.36
N		0.43		0.75		0.18
C		0.55		0.19		0.96
H		438 ppm		1,374 ppm		514 ppm

89-224-319a

36

7.2 Powder Production by the Plasma-Rotating Electrode Process (PREP)

Industrial Materials Technology (IMT) fabricated electrodes of each of the ten Ti-Li- and Ti-Mg-based alloys listed in Table 20. MDRL supplied 5 kg of constituent powders for each alloy. Because the tap density of the blended powders was only about 25%, IMT consolidated the powders by cold isostatic pressing (CIP) prior to HIP. Lithium reacted with the rubber bag used for CIP and caused leaks, but replacement silicone-rubber bags functioned satisfactorily. Three bags of each alloy were CIPed, and these compacts were then stacked inside 76-mm- (3-in.) diameter titanium tubes which were vacuum outgassed, sealed, and leak checked. HIP was performed at 1000°C and 105 MPa (15 ksi) for 8 h. Melt-through occurred in some of the cans during HIP. Alloys 11, 13, 14, 15, 16, and 18 appeared to be well consolidated, while alloys 12, 17, 19, and 20 were not fully compacted (see Figures 27a and b).

Table 20. Ti-Li and Ti-Mg based alloys selected for plasma-rotating electrode process (PREP) powder production study.

No.	Alloy
11	Ti-8Al-2Li
12	Ti-8Al-1Li-3Mg
13	Ti-8Al-2Li-1B-1C
14	Ti-8Al-1Li-3Mg-1B-1C
15	Ti-8Al-1Li-3Mg-1B-1C-1Si
16	Ti-26V-5Mg-3Li-1Al
17	Ti-26V-5Mg-3Li-1Al-1B-1C
18	Ti-26V-5Mg-3Li-3Al
19	Ti-26V-3Al-5Mg-1B-1C
20	Ti-26V-3Al-3Mg-1B-1C-1Li

89-224-320a

The HIP compacts were decanned, turned down to diameters of approximately 5.6 cm (2.2 in.), and then shipped to Nuclear Metals, Inc. for production of powder by the plasma rotating electrode process (PREP) (Reference 7). The first alloy attempted was no. 13 (Ti-8Al-2Li-1B-1C). The sample electrode was rotated at 10 000 rpm, but once the arc was established, chunks broke off and a dense white cloud erupted. Persistent development of this cloud required stopping the arc every 15 s and waiting until visibility was restored. Atomization of 10 cm of the electrode required 8 hours and resulted in 65 g of powder - a yield of about 1%. The size distribution of the powder is as follows: 10.2 g of -80 mesh, 14.2 g of -60 + 80 mesh, 14.8 g of -30 + 60 mesh, and 25 g of + 30 mesh.

Alloy 18 (Ti-26V-5Mg-3Li-3Al), which did not contain B, was atomized. The electrode did not break into chunks of material but clouding still occurred. Atomization for 8 h yielded 300 g of powder - a yield of about 4%. Alloy 11 (Ti-8Al-2Li) was atomized to obtain powder for chemical analysis. A yield of 90 g was obtained in a shortened run.

Table 21 presents the chemical analysis of the PREP powder runs. All three powders contained large amounts of O and H and had significant losses of Mg and Li.

(a)

(b)

89-224-298
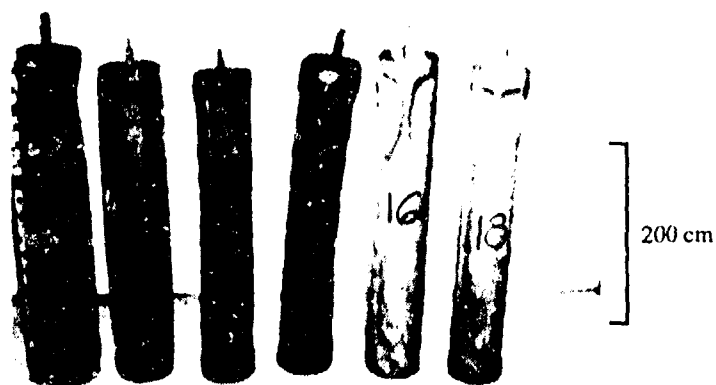
Figure 27. HIP compacts of (a) alloys 11, 13, 14, 15, 16, and 18
and (b) alloys 12, 17, 19, and 20 as received from IMT.

Table 21. Composition in weight percent of powder produced by PREP.
Target compositions are shown for comparision.

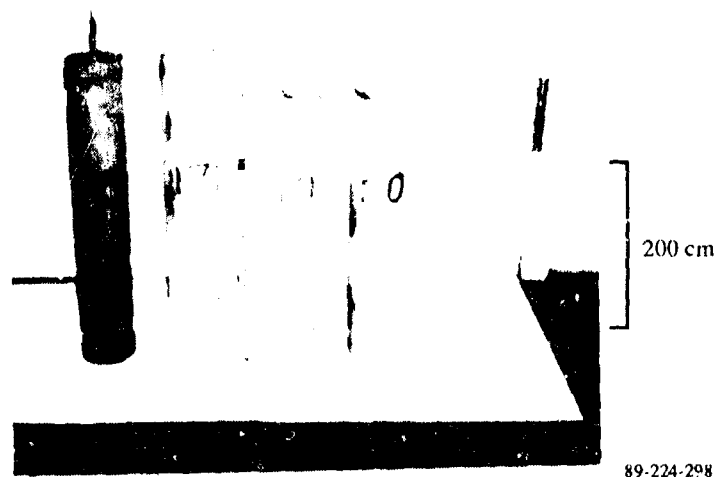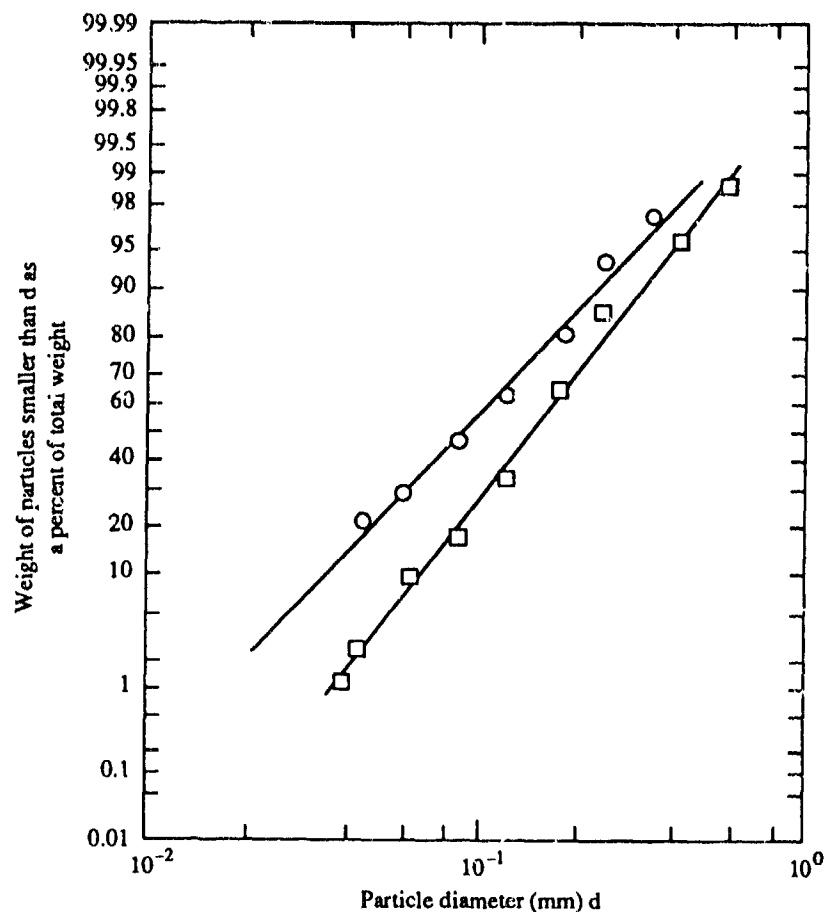| Alloying element	Alloy 11		Alloy 13		Alloy 18	
	Target composition weight %	Actual composition weight %	Target composition weight %	Actual composition weight %	Target composition weight %	Actual composition weight %
Al	8	8.12	8	8.18	3	3.25
Li	2	0.079	2	0.072	3	0.83
Mg					5	1.48
V					26	25.9
B			1	1.49		
O		0.92		1.02		1.00
N		0.022		0.021		0.097
C		0.091	1	0.40		0.15
H		223.7 ppm		180.3 ppm		784.6 ppm

89-224-321b

7.3 Powder Production by Induction Melting/Gas Atomization (IMGA)

The details of the IMGA facility at MDRL are described in Reference 8. The HIPed compacts from IMT were melted in an uncoated graphite crucible at the MDRL facilities. The sides of the compact were shielded from the crucible by a titanium liner, but the bottom was unshielded. The heating rate was accelerated (380°C/min) to minimize Li and Mg losses. Alloy 11 (Ti-8Al-2Li) was atomized initially with melt flow occurring at 1800°C. A powder yield of 215 g (28% yield) was obtained, and the inside of the chamber was covered with a fine white powder. Figure 28 shows that the particles from alloy 11 are much finer than those obtained in a typical production run for Ti alloys not containing Li (Reference 8). It is believed that vaporization of the Li particles is suppressed in the melt, but that this vaporization explodes the small droplets in the stream, thus leading to smaller particles. Alloy 12 (Ti-8Al-1Li-3Mg) was also atomized by this process with melt-flow initiating at 1350°C. Table 22 presents the chemical analysis of these IMGA alloys. The high level of C is expected since the charge was only partially shielded from the crucible. Substantial losses in Mg and Li occurred, although Li loss was much less in alloy 12, where flow was initiated at a lower temperature.

Attempts were then undertaken to obtain a melt flow at temperatures less than 1350°C to minimize lithium and magnesium losses. Attempts at induction melting at 1250 and 1300°C were made for a charge of HIPed compact Al alloy 12 (Ti-8Al-1Li-3Mg). The heating rate was accelerated (380°C/min) to minimize losses. However, no flow was attained at either of these temperatures. The IMGA apparatus was concluded to be unsuitable in its present configuration for producing Ti-Li-Mg alloy powder.

89-224-299

Figure 28. Particle size-distribution of (o) alloy 11 (Ti-8Al-2Li) obtained
from IMGA and (□) a typical titanium alloy not containing lithium. (Ref 8).

Table 22. Composition in weight percent of powder produced by IMGA.
Target compositions are shown for comparision.

| Alloying element	Alloy 11		Alloy 12	
	Target composition weight %	Actual composition weight %	Target composition weight %	Actual composition weight %
Al	8	6.9	8	6.04
Li	2	0.023	1	0.19
Mg			3	0.058
O		1.19		1.56
N		0.035		0.050
C		1.12		0.62
H		189 ppm		325 ppm

89-224-322b

8. CONCLUSIONS

Results of this study clearly demonstrate that Ti–Al–Be based alloys produced by rapid solidification and powder–metallurgical processing are attractive candidates for use in advanced aircraft structures and propulsion systems. The properties of the alloys are compared with program goals in Figures 29 and 30. The principal conclusions of this study are:

1. In spite of the large differences in melting points of Ti and Be, rapidly solidified powders containing the desired concentrations of Be can be produced consistently by the standard RSR technique.

2. Powders of Ti–6Al–4V–xBe and Ti–25V–xBe alloys can be extruded to fully dense rods at 900°C, a typical temperature for processing conventional Ti alloys. Powders of Ti–34Al–xBe can be extruded to fully dense rods at 1150°C; a temperature considerably lower than that required for extrusion of conventional TiAl based alloys.

3. The Ti–Be alloys can be machined by the same techniques used for the respective base alloys.

4. The as–extruded microstructures are fine grained (1–5 μm) and contain fine (10–20 nm) TiBe$_2$ precipitates. These microstructures can be coarsened by heat treating to enhance mechanical properties.

5. The Be additions modify the mechanical properties in the following ways:

A) Each 1 wt% addition of Be decreases the alloy density by 1.5%.

B) Each 1 wt% addition of Be increases the elastic modulus by 4 to 7%.

C) The Ti–Be alloys have high temperature strengths which are at least 50% greater than those of comparable alloys not containing Be (Figures 30a and b). At temperatures less than 800°C, Ti–6Al–4V–7Be has higher specific flow stresses than TiAl and Ti$_3$Al alloys.
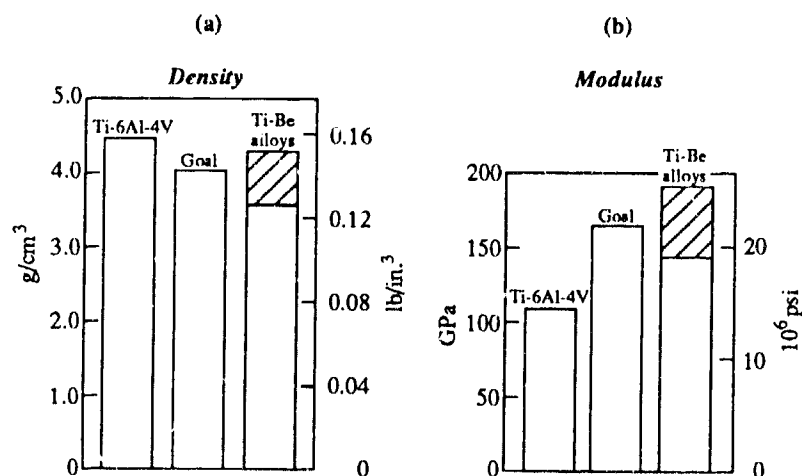
89-224-296b

Figure 29. Comparison of contract goals and experimental results of (a) density and (b) elastic modulus. Cross-hatched regions denote range of values of Ti-Be alloys.

(a)

Yield Strength

(b)

Elevated Temperature Strength
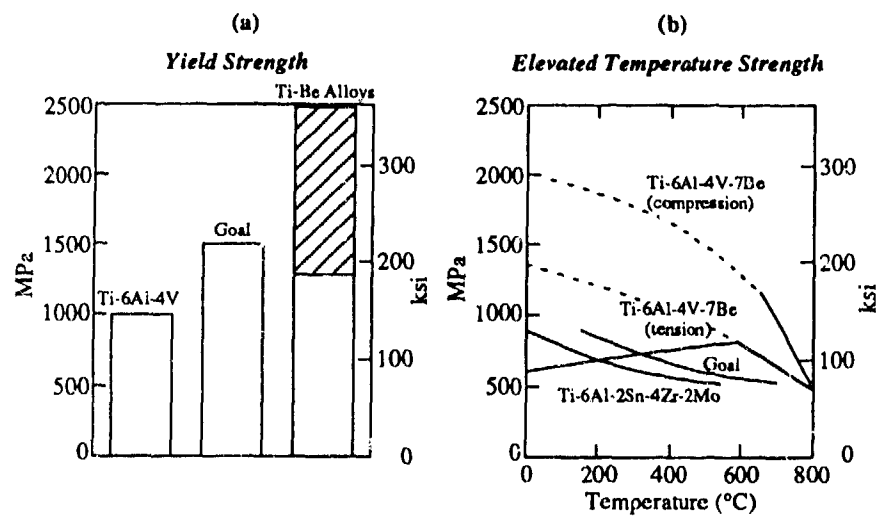
89-224-797b

Figure 30. Comparison of contract goals and experimental results of
(a) yield strength at 25°C and (b) elevated temperature strength.
Cross-hatched region denotes range of values of Ti-Be alloys.

9. SUGGESTIONS FOR FUTURE RESEARCH

9.1 Control of Interstitial Oxygen Concentration

This investigation demonstrated that additions of 4 to 7 wt% Be to titanium alloys effect significant reductions in density and improvements in modulus and result in excellent high-temperature strengths. However, the alloys prepared for this initial study had high interstitial-oxygen concentrations and were brittle at 25°C. This brittleness is probably caused by the combined effects of the high oxygen concentrations and the $TiBe_2$ dispersions; these effects need to be isolated to guide further alloy development.

The high oxygen concentrations, which were introduced during casting of the ingots, are attributed to the relatively poor vacuum of 40 Pa (0.3 Torr) during melting and casting and to the BeO wash used to protect the alumina crucibles from the melts. A vacuum system with lower background pressure will be required to minimize oxygen contamination from the environment. Complete melting of the Lockalloy rods and other alloying pieces was observed to occur around 1345°C, and the alloys were cast at 1425 to 1460°C. It is significant that in the subsequent powder-production operations, which were accomplished in uncoated graphite crucibles, the carbon and oxygen concentrations did not increase, even when the pour temperature was as high as 1325°C. The results indicate that graphite crucibles can be used for melting and casting of Ti-Be alloys at 1325-1350°C without risking carbon contamination.

9.2 Heat Treatment Optimization

Alloys should be heat-treated to produce variations in grain size and distribution, and in crystallographic texture. The mechanical properties should be evaluated to identify the heat treatment which gives the best combination of ambient- and elevated-temperature properties.

9.3 Microstructure/Property Correlations

The microstructures, phase distributions, and crystallographic textures of the matrix, and crystal structures and chemical compositions of fine precipitates, should be determined. The dislocation structures in deformed specimens should be determined to identify the role of Be in modifying deformations.

9.4 Oxidation Characterization

Since Be additions can affect oxidation resistance by several mechanisms, the oxidation rates and products, and concentration profiles should be determined to assess the effect of Be additions.

9.5 Superplastic Formability Evaluation

The alloys of the present program have fine microstructures which are stable at elevated temperatures. Thus they are expected to have good superplastic forming properties, which are necessary for many intended applications. The strain rate sensitivity, m, and total elongation should be determined as functions of temperature.

MDC QA028
15 April 1989

REFERENCES

1. Titanium Alloys Handbook, R. A. Wood and R. J. Favor, eds. (Metals and Ceramics Information Center, Battelle, Columbus, 1985).

2. J. L. Shade, Preliminary Material Properties of Titanium-Aluminides, AFWAL F33615-79-C-2091.

3. T. L. Mackay, S. M. L. Sastry, and C. F. Yolten, Metallurgical Characterization of Superplastic Forming, AFWAL-TR-80-4038.

4. S. M. L. Sastry, R. J. Lederich, and J. E. O'Neal, Optimum Microstructures for Superplastic Forming Using Hydrovac, AFWAL-TR-83- 4018.

5. Metals Handbook, 9th Edition (ASM, Metals Park, Ohio, 1980), vol. 3.

6. T. C. Peng, S. M. L. Sastry, and J. E. O'Neal, Laser Melting/Spin Atomization Method for the Production of Titanium Alloy Powders, Metall. Trans. 16 A, 1897 (1985).

7. P. R. Roberts and P. Lowenstein, Titanium Alloy Powders Made by the Rotary Electrode Process, in Powder Metallurgy of Titanium Alloys, F. H. Fries and J. E. Smugresky, eds. (TMS-AIME, New York, 1980).

8. B. London, T. C. Peng, and S. M. L. Sastry, Microstructural Studies of Rapidly Solidified TiAl Alloy Powders, 2nd International Conference on Rapidly Solidified Materials, San Diego, CA, 7-9 March 1988.

DISTRIBUTION LIST

Copies

Air Force Wright Aeronautical Lab.,Wrigth Patterson
AFB, OH 45433, W. Griffith (MLTM) and J. Kleek
(WL/MLLM)..2

ARPA, 3701 North Fairfax Drive, Arlington, VA 22203,
William Barker, Robert Crowe, Benn Wilcox............3

Allied-Signal Corp., P.O. Box 1021R, Morristown,
NJ 07960, S.K. Das....................................1

BDM International, Inc., 4001 N. Fairfax Dr. #750,
Arlington, VA 22203, P. A. Parrish...................1

Boeing Commercial Airplane, Seatle WA , W. Quist...........1

Center for Naval Analyses, 4401 Front Ave.,
P.O. Box 16263 Alexandria, VA 22302-0268.............1

Clemson University, Dept. of Mechanical Engineering,
Riggs Hall, Clemson, SC 29634-0921, H.J. Rack........1

Jeff Cook, 1233 N. Mesa Dr., Apt. 1140, Mesa Arizona
85201..5

Deiense Technical Information Center, Bldg. #5,
Cameron Station, Bldg. 5, Alexandria, VA 22314
(Attn. Adminstrator).................................2

Department of Energy, 100 Independence Av., SW
Washington, DC 20585, Code CE142.....................1

Drexel University, Dept. of Materials Engineering, 32nd
and Chestnut St., Phila., PA 19104. M. J. Koczak.....3

Grumman Areospace Corp., Bethpage, NY 11714,
M. Donnellan, P. N. Adler............................2

Innovare Inc., Airport Road, Commonwealth Park,
7277 Park Drive, Bath, PA 16014, Al R. Austen.......1

Lockheed Missiles and Space Co., Metallurgy Dept. 93-
10/204, 3251 Hanover St., Palo Alto CA 94304,
R. Lewis and J. Wadworth.............................2

Marko Materials Inc., 144 Rangeway Rd., N. Billerica,
MA 01862, R. Ray.....................................1

Martin Marietta Laboratories, 1450 South Rolling Rd.,
Baltimore. MD 21227-3898, J. Venables, K.S. Kumar....2

Metal Working News, 201 King of Prussia Rd., Radnor, PA
     19089, R. K. Irving...1

Metal Working Technology Inc. 1450 Scalp Avenue,
     Johnstown, PA 15904, W. L. Otto.........................1

McDonnell Aircraft Co., Box 516, Saint Louis, MO 63166,
     K. K. Sankaran...1

NASA Headquarters, 600 Independence Av., Washington,
     DC 20546, N. Mayer, S. Vennesi.........................2

NASA Langley Research Center, Hampton, VA 23365,
     A. Taylor, L. Blackburn, ...2

National Bureau of Standards, Gaithersburg, MD 20899,
     R. Shaffer, J. R. Manning.............................2

National Science Foundation, Office of Science and
     Technology Centers Division, 1800 G Street,
     Washington, DC 20550, L. W. Haworth...................1

NAWCADWAR, Warminster, PA, 18974-5000,
     Library, Code 8131 (2 Copies),
     W.E. Frazier, Code 6063 (10 Copies)..................12

NAVAIRSYSCOM, Washington, DC 20361, J. Collins Air-
     5304, L. Sloter Air-931...............................2

NAWCADWAR, Lakehurst, NJ 08733-5100, R. Celin (AV624-
     2173),R. Jablonski (AV624-2174), G. Fisher (SESD)
     (AV624-1179), B. Foor (02T) 4

NAWCADWAR, P.O. Box 7176, Trenton, NJ 08628-0176,
     F. Warvolis (PE34), A. Culbertson, ...2

Naval Air System Command, Washington, DC 20361-5140,
     R. A. Retta (AIR-51412), ...1

Naval Air System Command, Washington, DC 20361-5140,
     J. Jarrett (AIR-51412J),..............................1

Naval Industrial Resources Support Activity, Bldg. 75-2
     Naval Base Phila., PA 19112-5078, L. Plonsky
     (NAVIRSA-203)...1

Naval Post Graduate School, Mechanical Engineering
     Department, Monterey, CA 93943, T. McNelly...........1

Naval Research Laboratory, Washington, DC 20375,
     Metallurgy 1